Exploiting Successive Interference Cancellation for Spectrum Sharing over Unlicensed Bands

Zhiwu Guo, *Student Member, IEEE,* Ming Li, *Senior Member, IEEE,* and Marwan Krunz, *Fellow, IEEE*

Abstract—Harmonious coexistence among different unlicensed wireless technologies has became increasingly important due to the spectrum shortage problem. As a representative case, we focus on addressing LTE-LAA and WiFi coexistence in unlicensed bands. Traditionally, collision avoidance-based medium access control (MAC) protocols adopted by LAA and WiFi have led to low channel utilization and fairness. In this paper, we explore physical-layer interference suppression techniques (e.g., successive interference cancellation, SIC) to enhance the spectrum utilization of coexisting LAA and WiFi networks. We propose a SIC-aware MAC protocol that embraces concurrent transmissions and optimizes the channel access strategy at the MAC layer, so as to mitigate the cross-technology interference and improve spectrum efficiency and fairness. We theoretically analyze the network throughput by extending Bianchi's Markov model, considering the impact of concurrent transmissions and SIC. We also extend the analysis to consider MIMO and MU-MIMO links with SIC. We validate our theoretical analysis and the effectiveness of the proposed MAC protocol via extensive simulations. We also implement a prototype LAA/WiFi SIC receiver on USRP devices to demonstrate the feasibility of cross-technology SIC and the proposed MAC protocol.

Index Terms—Spectrum sharing, unlicensed bands, successive interference cancellation, LAA/WiFi coexistence, concurrent transmissions, MAC protocol, Markov analysis, USRP implementation.

1 Introduction

With the exponential growth of mobile devices and data, the licensed spectrum is becoming increasingly crowded to meet the demands of mobile data providers. To deal with this challenge, FCC proposed to enable LTE operators to extend their services into the 5 GHz unlicensed bands [1]. 3GPP also has ongoing efforts to extend 5G new radio (NR) to unlicensed bands at 5 GHz and 6 GHz [2]. Within this band, other unlicensed technologies, especially WiFi services are commonly deployed. Enabling cellular networks (e.g., LTE/5G NR) to harmoniously coexist with other unlicensed technologies has been a topic of intense study in both academia and industry. In this paper, we use LTE/WiFi coexistence as a representative scenario to study the potential benefit brought by interference cancellation techniques in unlicensed bands.

In 2013, Qualcomm proposed a duty-cycle (TDMA) based MAC protocol for LTE (i.e., LTE-U) [3] to operate in 5G unlicensed bands. Previous research [4] has shown that LTE-U will greatly affect the coexisting WiFi network's performance and lead to unfairness between the two networks. Thus, it is of great importance to develop an efficient spectrum sharing and transmission protocol to minimize the cross-technology interference between LTE and WiFi and achieve fair coexistence. 3GPP standardized LTE Licensed-Assisted Access (LAA) (i.e., LTE-LAA) as a global long-term solution for LTE/WiFi coexistence in unlicensed bands. To access the shared unlicensed spectrum, LTE-LAA adopts listen-before-talk (LBT) [5], which is similar to the carrier sense multiple access with collision avoidance (CSMA-CA) [6] in WiFi systems. Under LBT, an LAA [1] transmitter firstly conducts clear channel assessment (CCA) for a certain duration to check channel availability before transmission. If the channel is sensed idle, the LAA transmitter will transmit. In other words, by performing LBT in LAA networks and CSMS/CA in WiFi networks, collisions among LAA and WiFi can be generally avoided unless there are hidden terminals.

1.1 Motivation

Existing work on LAA/WiFi coexistence mainly focuses on developing fair channel utilization mechanisms between LTE and WiFi in a time-sharing manner. With the CSMA-CA or LBT mechanism, only one transmitter can access the channel at any given time within the same collision domain, resulting in inefficient channel utilization. This motivates us to allow concurrent transmissions for LAA/WiFi links, and adopt interference cancellation (IC) techniques to alleviate the interference (either within the same or across different wireless technologies), improving the LAA/WiFi throughput and fairness. In order to maximize the benefits of IC techniques at the network level (e.g., overall throughput or fairness), the physical layer and medium access need to be jointly considered. This further motivates us to propose an IC-aware MAC protocol that enables concurrent transmissions (instead of avoiding them) and optimizes the

• *All authors are with the Department of Electrical and Computer Engineering, University of Arizona, Tucson, AZ, 85721. E-mail: {zhiwuguo, lim, krunz}@email.arizona.edu*

Manuscript received March 28, 2022; revised December 8, 2022, accepted March 7, 2023. The authors thank the anonymous reviewers for their insightful feedback and Amir-Hossein Yazdani-Abyaneh's help in conducting USRP experiments. This work is partly supported by NSF grants (CNS-1564477 (CAREER), CNS-1731164 (SpecEES), 2229386, 1910348, 1822071) and by the Broadband Wireless Access & Applications Center (BWAC). Any opinions, findings, conclusions, or recommendations expressed in this paper are those of the author(s) and do not necessarily reflect the views of NSF.

1. For simplicity, we use LAA to represent LTE-LAA.

channel access strategy at the MAC layer, so as to mitigate the interference due to excessive channel contention brought by many coexisting links.

We demonstrate the potential throughput improvement of concurrent transmissions via a two-link coexistence scenario in Fig. 1, which is presented as a toy example to illustrate a real topology of LAA/WiFi coexistence. The transmission power of WiFi access point (AP) and LAA base station (BS) are set as 23 dBm [5], [6], which is around 0.2 Watts. The same transmission power of WiFi AP and LAA BS implies that they have a similar transmission range. In the real world, the transmission range of WiFi (hence LAA) links is around 100 meters [7].

We simulate the normalized throughput of both LAA and WiFi links, which can be regarded as channel utilization (fraction of time) for successful transmissions. The successful decoding SINR threshold is set to 10 dB, and the scenarios in Fig. 1(a)(b) have the same network topology. Under collision avoidance for both networks, the total normalized throughput is around 0.8, wherein the normalized throughput of WiFi and LAA links are 0.34 and 0.46, respectively, which are shown in Fig. 1(a). In Fig. 1(b), we allow concurrent transmissions for both links. Both receivers are able to decode their interested signals with successive interference cancellation (SIC). As a result, the total normalized throughput is increased from 0.8 to 1.31, and the normalized throughput of both links are improved.

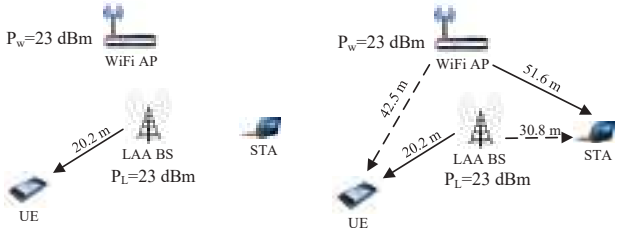

(a) Collision avoidance: $\text{thr}_W = 0.34, \text{thr}_L = 0.46, \text{thr}_{total} = 0.8$.

(b) Concurrent transmission with SIC: $\text{thr}_W = 0.61, \text{thr}_L = 0.70, \text{thr}_{total} = 1.31$.

Fig. 1: Toy example of two-link coexistence, successful decoding SINR threshold is 10 dB: (a) collision avoidance, (b) concurrent transmission with SIC.

1.2 Challenges

The above example only studies a simple and specific two-link coexistence topology. In general, for an arbitrary topology with multiple coexisting links possibly operating different technologies, it is challenging to quantify the benefits of concurrent transmission with IC techniques to the performance of coexisting networks. Furthermore, it is difficult to model and optimize the channel access strategies of coexisting networks (e.g., for each link, whether or when to transmit simultaneously with another link). Bianchi's Markov model [8] and its extensions (e.g., [9], [10]) were widely used to analyze the channel access behavior for contention-based MAC protocols where the back-off counter of each node is frozen upon detecting a busy channel (ongoing transmissions). Thus, classical Markov models were developed under the *collision-avoidance* paradigm. In order to generalize the traditional Markov model to consider the impact of concurrent transmissions and IC techniques, new analysis and modeling methods are required. This involves the characterization of successful decoding probabilities, and its impact on packet collision probabilities and throughput. In addition, not only the total throughput but also fairness must be considered as optimization objectives.

On the practical aspect, to realize such a concurrent transmission-enabled coexistence paradigm, a new MAC protocol needs to be developed, where nodes (links) make channel access decisions in a *distributed* manner, to achieve a certain optimized coexistence objective. However, in order to be compatible with existing LTE/WiFi protocol standards (or be integrated as an extension to current standards), minimal modifications to the current protocol are desired. This is a challenging goal, considering that the information needed for optimizing the concurrent channel access strategies can involve global topology and link interference relationships. Therefore, the channel access decision of one link can affect the transmission decisions of other links. If global network information is needed, it is undesirable to obtain it via explicit control message exchanges, since LAA and WiFi networks use two different technologies and protocols, which prevents direct communication between each other. To this end, information gathering via implicit sensing techniques is preferred. Finally, an implementation of SIC-based decoding across LAA and WiFi (which are heterogeneous networks) has not been done in the literature.

1.3 Contributions

Our contributions are summarized in the following:

(1) We propose a SIC-aware MAC protocol to enhance the coexistence of different wireless technologies in the unlicensed band (specifically, LAA and WiFi), which encourages concurrent transmissions instead of avoiding them.

(2) We provide a theoretical analysis of network throughput, by extending Bianchi's Markov model to consider contention at the concurrent transmission link set (CTS)-level, and model the impact of SIC on the collision probabilities. We also derive a general formula of successful decoding probabilities of multiple coexisting links using SIC-based decoding (in the same collision domain). Our analysis is also extended to consider MIMO and MU-MIMO with SIC.

(3) Based on the above analysis, we optimize the channel access strategy of the proposed MAC protocol in order to maximize network-level performance objectives (i.e., the total throughput or minimum link throughput (fairness)). For the protocol design, we introduce a training phase to discover the topology and learn the decoding performance of each CTS, without direct message exchanges between LAA and WiFi devices. In the transmission phase, all the links make optimized channel access decisions in a distributed manner. We also discuss practical issues such as overhead, node churn, and standards compatibility.

(4) We conduct extensive simulations to show the performance improvement of the proposed MAC protocol compared with two benchmarks: CSMA-CA and the optimal concurrent transmission strategy with capture effect (without SIC). We show that the network objectives of our protocol are significantly improved, for collision domains that include up to 5 concurrently transmitting links.

(5) We implement a prototype SIC receiver with USRP devices (for two-link coexistence), to demonstrate the feasibility of SIC decoding for LAA/WiFi coexistence. Experimental results show that the SIC receiver can successfully detect and decode both LAA and WiFi packets under a wide range of signal strength ratios between the two links (except when their signal strengths are very similar).

2 Background and Related Work

2.1 MAC Protocols for LAA/WiFi Coexistence

In this section, we review the MAC protocols used by WiFi and LAA networks and highlight their differences in contention and transmission parameters.

2.1.1 Overview of LAA/WiFi Channel Access Mechanism

WiFi systems adopt CSMA-CA to avoid collisions when multiple transmitters contend to access the same channel. LAA networks adopt LBT mechanism, which is similar to CSMA-CA. The state-of-the-art MAC protocols of LAA and WiFi are illustrated in Fig.2 for LTE/WiFi coexistence.

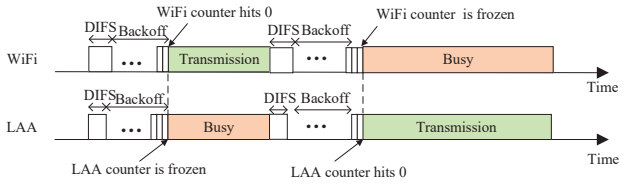

Fig. 2: Transmission timing diagrams of WiFi CSMA-CA (top) and LAA LBT (bottom) mechanism.

We use CSMA-CA adopted in WiFi as an example to illustrate the contention-based MAC protocol. Before each transmission, WiFi devices need to check if the channel is idle by performing carrier sensing (CS) for WiFi transmissions and energy detection (ED) for non-WiFi transmissions. CS and ED are conducted for a certain period which is known as distributed inter-frame spacing (DIFS). If the channel is sensed idle for DIFS duration, the WiFi transmitter will begin its back-off procedure. A back-off counter is generated uniformly from $[0, 2^j W_{\min} - 1]$, where j is the transmission stage, $W_{\min}$ is the minimum contention window. During the back-off process, the WiFi transmitter keeps monitoring the channel to check whether it is idle. If the channel is sensed busy, the WiFi device will freeze its back-off counter, and resume back-off once the channel is sensed idle for DIFS duration; if the channel is sensed idle after each MAC time slot σ, the back-off counter will be decremented by one. The WiFi transmitter starts transmission when its back-off counter hits zero. Once WiFi starts transmission, it can transmit for a duration called TXOP_w. Collision happens when the back-off counters of multiple transmitters hit zero at the same time slot, in which case the contention windows of collided transmissions will be doubled, namely $W_j = 2W_{j-1}$. However, there is a maximum contention window denoted as $W_{\max}$, namely $W_j = \min\{W_{\max}, 2^j W_{\min}\}$. The collided packets are retransmitted until reaching the maximum transmission limit.

2.1.2 LAA/WiFi Channel Access Parameters

Even though both WiFi and LAA networks contend to access the channel, they have different contention and transmission parameters. In Table 1, we summarize the main contention and transmission parameters of LAA and 802.11ac networks, both for the traffic class type I [5], [6].

TABLE 1: LAA/WiFi channel access parameters.

	DIFS	$W_{\min}$	$W_{\max}$	TXOP
LAA	25 μs	4	8	2 ms
802.11ac	34 μs	4	8	1.504 ms

2.2 Related Work

2.2.1 LAA/WiFi Performance Analysis

Most existing work of LAA/WiFi coexistence focused on collision avoidance-based fairness mechanism design. Cavalcante et al. [11] simulated LAA/WiFi coexistence and showed that the throughput of LAA is not affected much, while WiFi throughput is degraded greatly. Bianchi [8] provided a Markov model to compute the transmission probability and saturated throughput of 802.11 protocol. Based on Bianchi's approach, some works [9], [10], [12], [13], [14], [15] modeled the LAA/WiFi coexistence. Gao et al. [9] established a Markov model to calculate the throughput and delay of LAA/WiFi networks. The authors in [12], [13] investigated the throughput performance of different priority classes for LAA/WiFi coexistence, using the Markov model. Mehrnoush et al. [10] modified Bianchi's model to incorporate energy sensing threshold to evaluate the impact of threshold choices on the throughput performance. Yin et al. [14] adaptively adjusted the back-off window to satisfy the quality of service (QoS) of LAA networks while minimizing the collision probability of WiFi networks. The authors in [15] developed a model for the MAC delay distributions experienced by the WiFi packets and LTE frames. Xiao et al. [16] developed a modified back-of-the-envelope method for LAA nodes to evaluate their channel access probabilities when coexisting with other wireless technologies, such as WiFi. However, capture effect and concurrent transmissions were not considered in prior works.

2.2.2 Cross-Technology Interference Cancellation

Cross-technology interference cancellation (IC) has attracted significant interest recently [17], [18], [19], [20], [21]. Among these IC techniques, multiple input multiple output (MIMO) and successive interference cancellation (SIC) are mostly discussed. Gollakota et al. [17] presented technology independent multi-output (TIMO), a MIMO design that enables an 802.11n receiver to successfully decode the WiFi signal in the presence of a signal from a different technology by only measuring interference channel ratio information. Based on TIMO, Hou et al. [18] proposed cooperative interference mitigation (CIM) paradigm to make two or more heterogeneous networks cooperatively cancel or mitigate the interference to each other with MIMO capabilities. Yang et al. proposed ZIMO, which is a sink-based MIMO design for harmonious coexistence of ZigBee and WiFi networks with the goal of protecting the ZigBee data packets from being interfered by high-power cross-technology signals. ZIMO

exploits opportunities resulting from differences (transmit power, signal duration) between WiFi and ZigBee. Yun et al. [21] proposed concurrent transmissions of LTE and WiFi. It developed a new method to iteratively estimate both LTE and WiFi channels, utilizing the fact there are a small amount of LTE channels (around 0.875 MHz) in the frequency domain that are not interfered by WiFi. However, the receiver needs to have multiple antennas to decode LTE and WiFi signal. SIC [22] was proposed to decode multi-user signals in next-generation cellular networks where non-orthogonal multiple access (NOMA) is employed for multiple users to access the same RF channel. However, this technique is mostly adopted in homogeneous networks. In [20], SIC was adopted to enhance the coexistence of WiFi/ZigBee which are heterogeneous networks. Since the WiFi signal is typically much stronger than the Zigbee signal, a receiver can decode the WiFi signal and Zigbee signal successively using the SIC technique.

2.3 Overview of Successive Interference Cancellation

SIC is an effective technique for receivers to decode their own interested signals when multiple transmitted signals (from different sources) are superimposed. The basic idea of SIC is that received signals are decoded sequentially while canceling already decoded signals from interference. Specifically, the signal with the highest SINR (if it is equal to or greater than the minimum decoding SINR threshold) can be first decoded while treating other unknown weaker signals as noise. Then the signal with the second-highest SINR can be decoded after the cancellation of the already decoded strongest signal, and the above process continues iteratively until the desired signal is decoded.

The decodability in each step of SIC depends on the received signal strengths (RSS) as well as decoding SINR thresholds. Suppose there are K overlapped signals received by a Rx, the RSS from the highest to lowest are $S_1, S_2, \cdots, S_K$, respectively. Namely $S_1 > S_2 > \cdots > S_K$. The noise power in Rx is N_0. Rx will first decode the strongest signal S_1 [2] . The SINR when decoding S_1 is

$$\gamma_1 = \frac{S_1}{\sum_{i=2}^{K} S_i + N_0}. \tag{1}$$

To successfully decode S_1, suppose the minimum decoding SINR threshold of Rx is θ, γ_1 has to satisfy

$$\gamma_1 \geq \theta. \tag{2}$$

If Eq. (2) is satisfied, Rx can proceed to decode the second strongest signal S_2 by reconstructing S_1 and subtracting it from the received signal. The SINR when decoding S_2 is

$$\gamma_2 = \begin{cases} \dfrac{S_2}{\sum_{i=3}^{K} S_i + N_0}, & \text{if } K \geq 3 \\ \dfrac{S_2}{N_0}, & \text{if } K = 2 \end{cases} \tag{3}$$

If $\gamma_2 \geq \theta$, Rx can successfully decode S_2, other signals can be decoded following the similar process.

2. We abuse notation slightly and use S both for the received signal S and for its signal power.

3 System Model and Illustrative Example

3.1 System Model

We consider a multi-link LAA/WiFi coexistence model as shown in Fig. 3(a), where there are N_W WiFi links and N_L LAA links. All links coexist in the same area and share the same 5 GHz unlicensed band. Each node has either a single antenna or multiple antennas. Without loss of generality, we focus on the downlink transmissions under saturated traffic conditions. Our basic system model assumes that at any time instance, each WiFi AP serves one station (STA) and each LAA BS serves one user equipment (UE). This assumption is only needed for simplifying our analysis, which can be easily generalized to frequency-division systems.

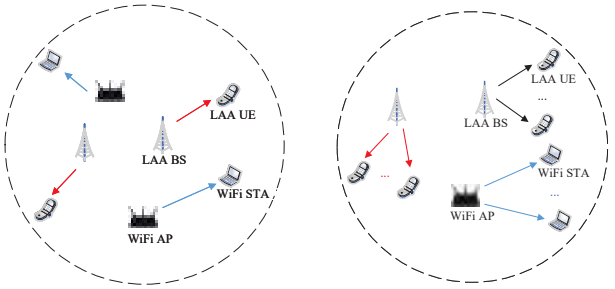

(a) Basic system model: multi-link LAA/WiFi coexistence. Each node has either a single antenna or multiple antennas.

(b) Multi-link LAA/WiFi coexistence with MU-MIMO.

Fig. 3: System models.

We assume a cross-technology IC technique is adopted by each coexisting link. In this paper, we focus on SIC, which does not require multi-antenna capability. Thus, we will begin our analysis by assuming single-antenna nodes, then extend it to MIMO and multi-user MIMO (MU-MIMO) scenarios in Fig. 3(b), which will be analyzed in Sec. 6. Note that, other interference cancellation techniques can also be integrated, such as MIMO-based IC[3].

3.2 Illustrative Example

We showcase a three-link coexistence scenario in Fig. 4 to illustrate the potential advantages brought by concurrent transmissions across LAA and WiFi links, which motivates our MAC protocol design. In Fig. 4, there are two WiFi links and one LAA link coexisting in a $50 \times 50\ m^2$ area. We simulate with the LAA/WiFi channel access parameters given in Table 1 and assume each receiver is SIC-capable. Rayleigh channel model is considered for each link. The successful decoding SINR threshold of three links are set as 10 dB. The successful decoding probabilities for all possible transmission strategies are shown in Table 2, defined as the ratio of the number of successfully decoded packets to the total number of transmitted packets. Compared with the traditional collision avoidance strategy, concurrent transmissions

3. For example, TIMO [17] and Yun and Qiu's scheme [21] for cancelling cross-technology interference. Lin et al. proposed a MIMO IC-based MAC protocol [23] for WiFi networks. We can combine them to design an optimized MAC protocol for MIMO IC across different technologies. This will be a future work.

TABLE 2: Successful decoding probability and normalized throughput of each possible transmission strategy.

Possible transmission strategies	Successful decoding probability			Normalized throughput			
	link 1	link 2	link 3	link 1	link 2	link 3	total
Collision avoidance	1	1	1	0.22	0.22	0.30	0.74
Link 3 transmits alone, links 1 and 2 concurrently transmit	0.27	0.20	1	0.17	0.13	0.37	0.67
Link 2 transmits alone, links 1 and 3 concurrently transmit	0.38	1	0.32	0.18	0.26	0.26	0.70
Link 1 transmits alone, links 2 and 3 concurrently transmit	1	0.28	0.96	0.21	0.17	0.49	0.87
Links 1, 2, and 3 concurrently transmit	0.08	0.04	0.30	0.08	0.04	0.30	0.42

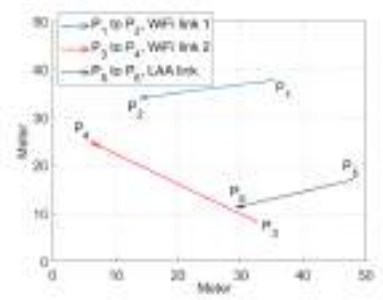

Fig. 4: Three-link coexistence scenario.

may increase (or decrease) the successful decoding probabilities of concurrent links, which further impact their throughput. For example, for the transmission strategy that link 1 transmits alone, link 2 and link 3 concurrently transmit, the successful decoding probability of link 3 is 96%, which is close to 1. However, link 2 only has a successful decoding probability of 28%. We further show the impact of successful decoding probabilities on the normalized throughput (or channel utilization) under different transmission strategies in Table 2. For the transmission strategy that link 1 transmits alone while link 2 and 3 concurrently transmit, the total throughput is improved from 0.74 to 0.87, compared with collision avoidance transmission strategy.

4 Concurrent Transmission Enabled MAC Protocol for LAA/WiFi Coexistence

In this section, we give an overview of the design principles, necessary definitions, and details of the transmission phase of our MAC protocol. This can help us model and analyze its performance in Sec. 5.

4.1 Overview of Proposed MAC Protocol

The high-level design principle of the proposed MAC protocol is to allow concurrent transmissions of multiple LAA/WiFi links. Specifically, the set of links that can concurrently transmit is called a CTS (see Definition 1 below). The set of CTSes is called a TS (see Definition 2), which is to be optimized (presented in Sec. 7). We assume all the CTSes in a TS are disjoint sets, i.e., each link belongs to only one CTS. Channel access contention happens at the CTS level, where a CTS is regarded as a whole entity. The CTS level contention model is different from CSMA-CA, where contention happens at link level. The implementation of CTS-level contention can vary in practice, e.g., only one representative link contends channel access on behalf of the CTS, or any link can contend.

To model the concurrent transmissions of the coexisting links, we define *concurrent transmission set (CTS)* as follows:

Definition 1 (CTS). A Concurrent Transmission Set (CTS) is a set of links with overlapping transmissions. Specifically, if any one of links in the set wins channel contention and starts transmission, other links in the same CTS will start transmissions once detecting the ongoing transmission. Therefore, all links in a CTS always concurrently transmit [4].

Remark 1: For the scenario of N total coexisting LAA/WiFi links, there are $2^N - 1$ possible CTSes.

Besides the definition of CTS, we define *transmission strategy (TS)* in the following, which aims to model how different CTSes are chosen in the proposed MAC protocol.

Definition 2 (TS). A Transmission Strategy (TS) is a set which consists of one or multiple CTSes. In addition, we restrict all CTSes in a TS to be disjoint sets and each link must belong to one CTS in a TS.

For the scenario of three-link coexistence as shown in Fig. 4, according to the definition of TS, there are five TSes: $\text{TS}_1 = \{\{1\},\{2\},\{3\}\}$; $\text{TS}_2 = \{\{1\},\{2,3\}\}$; $\text{TS}_3 = \{\{2\},\{1,3\}\}$; $\text{TS}_4 = \{\{3\},\{1,2\}\}$; $\text{TS}_5 = \{\{1,2,3\}\}$. The numbers in the above TSes represent link indices. For example, $\text{TS}_3 = \{\{2\},\{1,3\}\}$ means that there are two CTSes in TS_3, CTS_1 is link 2, CTS_2 consists of link 1 and link 3. We can see that, in each TS, each link is active in only one CTS of a given TS. TS_1 is the transmission strategy of collision avoidance since links 1, 2, and 3 transmit alone (i.e., belong to different CTSes).

We restrict that each link only belongs to one CTS for a given TS, because allowing each link belonging to multiple CTSes will significantly complicate the MAC protocol design. The number of TSes would increase to the order of 2^{2^N-1} for the N link coexistence scenario. Since the goal of the our MAC protocol is to select the optimal TS to achieve a certain network objective, a large number of TSes will also increase the computation overhead of the optimization process. Besides, given a specific coexistence topology, not all links can benefit from concurrent transmissions.

Remark 2: For the scenario of N coexisting LAA/WiFi links, denote the number of TSes as B_N. According to the partition of a set [24], B_N can be obtained through the following recursive expression:

$$B_N = \sum_{k=0}^{N-1} \binom{N-1}{k} B_k, \text{ with } B_0 = 1. \tag{4}$$

According to Eq. (4), we have $B_1 = 1, B_2 = 2, B_3 = 5, B_4 = 15, B_5 = 52, B_6 = 203$, etc.

As the channel contention of the proposed MAC protocol happens at CTS level, we define *CTS-level collision*:

4. We ignore the processing time of detecting ongoing transmission and treat transmissions in the same CTS as concurrent transmissions.

Definition 3 (CTS-level collision). Collision of $\text{CTS}_i \in \text{TS}$ happens under one of the following two cases: (1) there exists another $\text{CTS}_j \in \text{TS}$ that concurrently transmits with CTS_i; (2) all concurrent transmitting links in CTS_i fail to decode their desired signals.

Even though concurrent transmissions of multiple CTSes essentially form another bigger CTS (e.g., $\text{CTS}_{\text{new}} = \{\text{CTS}_i, \text{CTS}_j\}$), according to the simulation results shown in Fig. 11, the successful decoding probability of each link diminishes as the number of concurrent transmissions increases. Similar results were also obtained in [25], [26], which justify criterion (1) in the above definition. Furthermore, as we treat $\text{CTS}_i \in \text{TS}$ as an indivisible contention entity, successful decoding of any link in CTS_i resets CTS_i's contention window [5], criterion (2) in the above definition is consistent with the intuition of collisions in Fig. 6.

4.2 Transmission Phase of Proposed MAC Protocol

In this subsection, we show the detailed steps of the proposed concurrent transmission MAC protocol from the perspective of link $j \in \text{CTS}_i$, assuming a prior TS is given. We remark that the MAC protocol is conducted in a distributed manner.

As we treat $\text{CTS}_i \in \text{TS}$ as an indivisible contention entity, each CTS should reset or double its contention window based on CTS-level successful or collided transmission. According to Definition 3, CTS-level collision is related to successful or unsuccessful transmission information of all concurrent transmitting links in the same CTS. How could each link in the same CTS obtain this information in the transmission phase? To avoid communication overhead across LAA and WiFi links, each CTS can assign one link as the representative link, to contend with other CTSes. Intuitively, resetting CTS_i's contention window more frequently can benefit the long-term channel access of CTS_i. Therefore, for all links belonging to $\text{CTS}_i \in \text{TS}$, we select the link that has the highest successful decoding probability as the representative link for CTS_i to contend with other CTSes. Denote the representative link for CTS_i as link L_i. We present the detailed steps of the proposed MAC protocol from the perspective of link j, $j \in \text{CTS}_i$.

- **Step 1:** If link j is the representative link L_i (e.g., $j = L_i$), link j randomly generates a back-off counter BO_j based on its current contention window; Otherwise, it proceeds to step 4;
- **Step 2:** Link j contends channel access, if its sensed energy is lower than CCA_j, which is the energy detection threshold of link j to determine channel availability, BO_j is decreased by 1 every MAC time slot; Otherwise, BO_j freezes;
- **Step 3:** Link j accesses the channel when BO_j is equal to 0, it proceeds to step 5;
- **Step 4:** Link j senses the channel and accesses the channel when detecting the transmission of link L_i;
- **Step 5:** Link j finishes its transmission, returns to step 1.

5. For the purpose of practical MAC protocol implementation and analysis, we select only one link in each CTS to participate in the channel contention with other CTSes.

4.3 Illustrative Example of Proposed MAC Protocol

In Fig. 5, we illustrate the basic idea of the proposed MAC protocol for the topology shown in Fig. 4. Specifically, we show the MAC protocol of transmission strategy that link 1 transmits alone, link 2 and link 3 always transmit concurrently, namely $\text{CTS}_1 = \{1\}$, $\text{CTS}_2 = \{2, 3\}$. For CTS_2, either link 2 or link 3 can be the representative link. Therefore, either link 2 or link 3 can win the channel contention on behalf of CTS_2.

At time t_1, link 1 wins the channel contention and starts transmission. After link 1 finishes its transmission, followed by the DIFS period and back-off process, link 2 wins the channel contention at t_2. After that, link 3 detects the transmission of link 2. According to the transmission strategy, it will transmit concurrently with link 2. Similarly, if link 3 wins the channel contention at t_3, link 2 will also concurrently transmit with link 3. The MAC protocol in Fig. 5 is still contention-based. However, different from the collision avoidance-based MAC protocol shown in Fig. 2, it allows concurrent transmissions of multiple links (that are deemed beneficial with concurrent transmissions and SIC decoding). In this way, the total channel utilization or fairness among different links can be improved if optimal concurrent transmission strategies are identified and implemented.

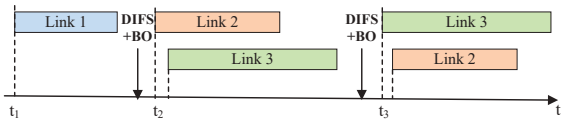

Fig. 5: Contention-based MAC protocol of three-link coexistence scenario, where concurrent transmissions of multiple links (e.g. link 2 and link 3) are allowed.

5 Markov-based Throughput Analysis

For a given TS, we quantify the benefit of concurrent transmissions with IC techniques to the performance of coexisting networks.

5.1 CTS-level Markov Analysis

We generalize the original link-level Markov model [8] to CTS-level Markov model. The corresponding link-level channel contention parameters are also changed to CTS-level counterparts, e.g., link-level channel access probability is adapted to CTS-level channel access probability. The goal of analysis is to quantify the effects of concurrent transmissions and SIC on the CTS-level collision probability. The key idea of our analysis is to treat each CTS as a whole (like an indivisible block of links) in terms of contention and calculate collision probabilities of different CTSes.

Fig. 6 depicts the CTS-level Markov model, where each contention parameter is CTS-level. In what follows, we analyze the channel access probability and collision probability of each CTS, under a given TS. Denote the channel access probability of $\text{CTS}_i \in \text{TS}$ as τ_i, which is the probability that CTS_i transmits in any contention time slot, the CTS-level collision probability of CTS_i as p_{ci}. Based on the relationship

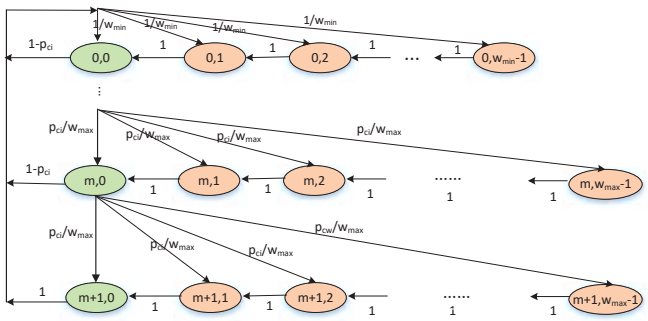

Fig. 6: CTS-level Markov model.

of transition probabilities for different states and the fact that the summation of stationary probabilities of all states is equal to 1, we can obtain τ_i as a function of p_{ci} [10]:

$$\tau_i = \frac{2}{W_{\min}\left(\frac{(1-(2p_{ci})^{m+1})(1-p_{ci})+2^m(p_{ci}^{m+1}-p_{ci}^{m+2})(1-2p_{ci})}{(1-2p_{ci})(1-p_{ci}^{m+2})}\right)+1}, \tag{5}$$

where $m = \log_2(\frac{W_{\max}}{W_{\min}})$.

As τ_i and p_{ci} are coupled with each other for CTS_i, we need to derive another equation for τ_i and p_{ci}. To analyze p_{ci}, we first analyze the successful decoding probability of each link under the concurrent transmission of all links in a given CTS (e.g., CTS_i), assuming that each receiver is SIC-capable.

5.2 Link-level Successful Decoding Probability of SIC for a Given CTS

Weber et al. [27] developed a closed-form of the transmission capacity (the maximum number of successful transmissions such that the outage probability does not exceed some specified threshold) of ad hoc networks with SIC receivers. However, it only considered path loss attenuation effects and ignored small-scale channel effects. The authors in [25], [26] derived a closed-form upper and lower bound for the probability of successively decoding k users. However, the SIC receiver has multiple interested signals, instead of one specific desired signal.

Consider a scenario where multiple transmitters from a given CTS concurrently transmit to one receiver. With SIC enabled in the receiver, we obtain the successful decoding probability of one specific interested signal in this subsection. We assume a Rayleigh channel model which is commonly used for LAA and WiFi networks and generalize the two-link coexistence scenario in our previous work [28] to multi-link coexistence scenario.

Generally, assume there are N concurrently transmitting links in total (SIC focuses on SINR of each link, thus the analysis of SIC applies to coexistence scenarios of any technology). Denote $\mathcal{N}$ as the set of all concurrently transmitting links, the transmitted signal of link i as x_i, and the RSS of x_i as s_i. Assume x_i is the interested signal for the SIC receiver. Before decoding x_i, all links with higher RSS than s_i need to be successfully decoded first. Therefore, all RSS order combinations related to s_i need to be considered. Define

$$O_{\mathcal{N}} = \{s_{l_1} > s_{l_2} > \cdots > s_{l_{k-1}} > s_i > \mathcal{RS}\}, \tag{6}$$

which is one ordered RSS list from the perspective of s_i (RSS of the interested signal), wherein $l_1, l_2, \cdots, l_{k-1}$ are link indices that have higher RSS than s_i, $\mathcal{RS} = \{s_j, j \in \mathcal{N}/\{l_1, l_2, \cdots, l_{k-1}, i\}\}$, which is residual set that consists of remaining weaker RSS, compared with s_i. Note that $\mathcal{RS}$ is not ordered since the SINRs of them do not impact the decoding of x_i.

Remark 3: Denote $P(n, r)$ as the number of permutations of selecting r objects from n objects at a time, which is $P(n, r) = \frac{n!}{(n-r)!}$. If link i is the strongest signal among link set $\mathcal{N}$, there are $P(N-1, 0)$ (which is equal to 1) possible RSS order lists for $O_{\mathcal{N}}$; if link i is the second-strongest signal among $\mathcal{N}$, there are $P(N-1, 1)$ RSS order lists for $O_{\mathcal{N}}$. Combining all possible cases from link i being the strongest signal to the weakest signal among $\mathcal{N}$, and denote the set of all RSS orders as $\Omega_{\mathcal{N}}$, we can obtain the cardinality of $\Omega_{\mathcal{N}}$, which is $|\Omega_{\mathcal{N}}| = \sum_{k=0}^{N-1} P(N-1, k)$.

Next, we calculate the probability of successfully decoding x_i from concurrent transmissions of link set $\mathcal{N}$. Denote $O_{\mathcal{N},r}, r = 1, 2, \cdots, |\Omega_{\mathcal{N}}|$ as the r-th RSS order list among $\Omega_{\mathcal{N}}$, $E_{O_{\mathcal{N},r}}(i)$ as the event of successfully decoding x_i under the specific RSS order $O_{\mathcal{N},r}$. Combining all possible cases of $O_{\mathcal{N},r}, r = 1, 2, \cdots, |\Omega_{\mathcal{N}}|$, the probability of successfully decoding x_i can be represented as:

$$\sum_{O_{\mathcal{N},r}, r=1}^{|\Omega_{\mathcal{N}}|} \mathbb{P}\Big(E_{O_{\mathcal{N},r}}(i)\Big). \tag{7}$$

$\mathbb{P}\Big(E_{O_{\mathcal{N},r}}(i)\Big)$ is derived in Appendix A of the supplemental material of this paper. The general formula of $\mathbb{P}\Big(E_{O_{\mathcal{N},r}}(i)\Big)$ is also given in Appendix B of the supplemental material of this paper.

5.3 CTS-Level Collision Probability under a Given TS

In this subsection, we analyze the impact of concurrent transmissions and SIC on the CTS-level collision probabilities in the CTS-level Markov model.

Mathematically, consider a given TS, we analyze the collision probability of each CTS in this TS. As discussed in Sec. 5.1, we need to obtain another equation for τ_i and p_{ci}, which is obtained in the following.

Assume at time t, the representative link L_i of CTS_i wins channel contention and accesses the channel. According to Definition 3, there are two cases that lead to the collision for the transmission of CTS_i. The first case is that at least one of the other CTSes accessing the channel at the same time slot (i.e., t) with CTS_i, which happens with a probability of $(1-\prod_{j\neq i, \text{CTS}_j \in \text{TS}}(1-\tau_j))$; the second case is that all the links in CTS_i fail to decode their interested signals. As we select the link that has the highest successful decoding probability as the representative link for CTS_i, the second case happens with probability $\Big(1-\max_{k\in\text{CTS}_i} p^s_{\text{CTS}_i}(k)\Big)\prod_{j\neq i, \text{CTS}_j\in\text{TS}}(1-\tau_j)$, where $p^s_{\text{CTS}_i}(k)$ is the successful decoding probability of link $k \in \text{CTS}_i$. Combining the above two cases, p_{ci} can be obtained as:

$$\begin{aligned} p_{ci} = &\Big(1 - \prod_{j\neq i, \text{CTS}_j\in\text{TS}} (1-\tau_j)\Big) \\ &+ \Big(1-\max_{k\in\text{CTS}_i} p^s_{\text{CTS}_i}(k)\Big) \prod_{j\neq i, \text{CTS}_j\in\text{TS}} (1-\tau_j). \end{aligned} \tag{8}$$

In summary, we have derived an additional equation for each CTS. Denote Q as the number of CTSes in TS. There are $2*Q$ unknown variables and $2*Q$ equations, which are coupled together. Thus, we can solve this system of equations numerically (e.g., using *fsolve* function in MATLAB).

5.4 Normalized Throughput of Each Link

The normalized throughput of LAA (or WiFi) is defined as the ratio of time occupied by the successful LAA (or WiFi) transmissions to the interval between two consecutive CTS-level transmissions [29].

Denote the transmission duration of WiFi and LAA links as T_W, T_L, respectively. The transmission duration of CTS_i is denoted as T_i, which is obtained as follows:

$$T_i = \begin{cases} T_L, \text{if there exists one LAA link in CTS}_i, \\ T_W, \text{Otherwise.} \end{cases} \tag{9}$$

To obtain the average interval between two consecutive transmissions of CTSes, three events are considered: collision-free transmissions of different CTSes (E_1), backoff during contention phase (E_2), collided transmissions of different CTSes (E_3). For E_1, it means there is only one CTS in transmission. From the perspective of CTS_i, it happens with probability $\tau_i \prod_{j\neq i, \text{CTS}_j \in \text{TS}}(1-\tau_j)$, the event duration is T_i. The probability of E_2 is $\prod_{\text{CTS}_i \in \text{TS}}(1-\tau_i)$, and the event duration is the MAC time slot σ. For E_3, there are multiple CTSes concurrently transmitting at the same time, therefore E_3 is the complementary of $E_1 \cup E_2$, which happens with the probability of $\Big(1 - \sum_{i=1}^{Q} \tau_i \prod_{j\neq i, \text{CTS}_j \in \text{TS}}(1-\tau_j) - \prod_{\text{CTS}_i \in \text{TS}}(1-\tau_i)\Big)$, where Q is the number of CTSes in TS. Due to the large combinations (i.e., $2^Q - 1 - Q$) for concurrent transmissions of multiple CTSes, we approximate the event duration of E_3 as $\max\{T_W, T_L\}$, which is the worst case in this situation.

Combing E_1, E_2, E_3 together, the average interval between two consecutive transmissions of CTSes can be obtained as:

$$\begin{aligned} T_{\text{int}} = &\sum_{i=1}^{Q} T_i \cdot \tau_i \prod_{j\neq i}(1-\tau_j) + \sigma \cdot \prod_{i}(1-\tau_i) \\ &+ \max\{T_W, T_L\} \cdot \Big(1 - \sum_{i=1}^{Q} \tau_i \prod_{j\neq i}(1-\tau_j) - \prod_{i}(1-\tau_i)\Big). \end{aligned} \tag{10}$$

Next, we obtain the average duration of successful transmission for each link during two consecutive CTS-level transmissions. Define the transmission duration of link $k \in \text{CTS}_i$ as:

$$D_k = \begin{cases} T_L, \text{if link } k \text{ is an LAA link}, \\ T_W, \text{Otherwise.} \end{cases} \tag{11}$$

Since each link only belongs to one CTS as we have defined, the average duration of successful transmission for link $k \in \text{CTS}_i$ during two consecutive CTS-level transmissions can be obtained as:

$$\Delta_k = D_k \cdot p^s_{\text{CTS}_i}(k) \cdot \tau_i \prod_{j\neq i, \text{CTS}_j \in \text{TS}} (1-\tau_j). \tag{12}$$

Therefore, the normalized throughput of link $k \in \text{CTS}_i$ is obtained as:

$$\text{thr}(k) = \frac{\Delta_k}{T_{\text{int}}}. \tag{13}$$

6 Extensions to MIMO and MU-MIMO

MIMO was introduced by 802.11n (WiFi 4) standard to increase the throughput of wireless networks. Based on MIMO, 802.11ac (WiFi 5) firstly adopted multi-user MIMO in WiFi systems, facilitating the concurrent transmission of different data streams to multiple user stations [6]. For LTE networks, MIMO/MU-MIMO scheme have also been identified as key technologies to achieve high spectral efficiency [5]. In this section, we discuss how to extend the previous single-antenna SIC analysis to MIMO and MU-MIMO scenarios. The analysis of the single-user MIMO without/with SIC cases are shown in the supplemental material.

6.1 Multi-user MIMO without SIC

In Fig. 3(b), we illustrate a generalized system model in the MU-MIMO setting, where each WiFi AP or LAA base station serves multiple users. Without loss of generality, we assume each WiFi AP and LAA BS are equipped with M antennas, serving K single-antenna STAs or UEs ($K \leq M$). To help us model this case, we propose a concept of *super link*, which is defined below.

Definition 4 (Super link). A super link is a (downlink) MU-MIMO link consisting of a WiFi AP or LAA BS and all the individual users associated with it. If a WiFi AP or LAA BS wins the channel contention, all the individual links that belong to the super link concurrently transmit.

We analyze the successful decoding probability of each MU-MIMO super link considering following two situations. If capture effect [30] is not considered, each MU-MIMO super link alone should be treated as one CTS since concurrent transmissions of multiple super links result in unsuccessful decoding (i.e., successful decoding probability is zero) for all the super links. In this situation, the analysis is similar to collision avoidance and we can adopt the similar analysis in Sec. 5 to obtain the throughput, with each MU-MIMO super link alone being one CTS. However, if capture effect is considered, the successful decoding probabilities of multiple MU-MIMO super links are between 0 and 1. In this situation, multi-user MIMO without SIC is a special case of multi-user MIMO with SIC. The difference is that, without SIC, the strongest signal can only be the interested signal for successful decodings. Therefore, the analysis is similar to multi-user MIMO with SIC, which is presented below.

6.2 Multi-user MIMO with SIC

We illustrate the signal model of MU-MIMO with SIC in Fig. 7, where there are N concurrently transmitting MU-MIMO super links. The super link associated with WiFi AP 1 is the interested signal.

We focus on the received signal components of WiFi STA $k (1 \leq k \leq K)$ within the first super link. Denote $\mathbf{h}_{i,k} \in \mathbb{C}^{1\times M}$ as the channel vector from transmitter $i (1 \leq i \leq N)$ to WiFi STA k. Denote the link set in super link i as $\mathcal{S}_i$ and $\mathbf{w}_{i,l} \in \mathbb{C}^{M\times 1}$ as the transmit precoding vector from

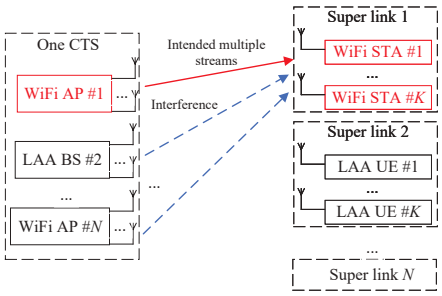

Fig. 7: Signal model of MU-MIMO with SIC.

transmitter i to user $l \in \mathcal{S}_i$. $s_{i,l}$ is the normalized transmit symbol from transmitter i to user $l \in \mathcal{S}_i$. $n_{1,k}$ is the white Gaussian noise. Therefore, the received signal at WiFi STA $k(k \in \mathcal{S}_1)$ can be represented as

$$y_k = \mathbf{h}_{1,k}\mathbf{w}_{1,k}s_{1,k} + \sum_{k' \in \mathcal{S}_1} \mathbf{h}_{1,k'}\mathbf{w}_{1,k'}s_{1,k'} + \sum_{i,i\neq 1} \mathbf{h}_{i,k} \sum_{l \in \mathcal{S}_i} \mathbf{w}_{i,l}s_{i,l} + n_{1,k}. \quad (14)$$

The first term, second term, and third term of right-hand side of Eq.(14) represent the interested signal, other signals from the same super link, and other signals from different super links, respectively. We assume the nodes adopt Zero-forcing beamforming (ZFBF) [31], which is widely used in MU-MIMO to enable multi-user concurrent transmission by creating orthogonal channels and removing the cross-user interference in the same super link. Therefore, Eq.(14) can be further written as

$$y_k = \mathbf{h}_{1,k}\mathbf{w}_{1,k}s_{1,k} + \sum_{i,i\neq 1} \mathbf{h}_{i,k}\mathbf{x}_i + n_{1,k}, \quad (15)$$

where $\mathbf{x}_i \in \mathbb{C}^{M\times 1}, \mathbf{x}_i = \sum_{l\in\mathcal{S}_i} \mathbf{w}_{i,l}s_{i,l}$ is the transmit signal vector of transmitter i. We can obtain the SINR from transmitter i to WiFi STA k $(k \in \mathcal{S}_1)$ as:

$$\text{SINR}_{i,k} = \begin{cases} \dfrac{||\mathbf{h}_{1,k}\mathbf{w}_{1,k}||^2}{\sum_{j,j\neq 1} ||\mathbf{h}_{j,k}\mathbf{x}_j||^2 + N_0}, \text{if } i = 1, \\ \dfrac{||\mathbf{h}_{i,k}\mathbf{x}_i||^2}{||\mathbf{h}_{1,k}\mathbf{w}_{1,k}||^2 + \sum_{j,j\neq i} ||\mathbf{h}_{j,k}\mathbf{x}_j||^2 + N_0}, \text{Otherwise.} \end{cases} \quad (16)$$

Comparing $\text{SINR}_{i,k}, 1 \leq i \leq N, k \in \mathcal{S}_1$, we can obtain the strongest super link which has the largest SINR. After decoding and canceling the strongest super link, we further obtain the second-strongest super link, the above process continues iteratively until the desired signal is decoded. Therefore, the SIC decoding order for the scenario of multi-user MIMO with SIC can be obtained.

We remark that the above analysis assumes the channels are deterministic. To obtain the successful decoding probability of SIC under stochastic channels, the RSS distribution of signals (i.e., $\mathbf{h}_{1,k}\mathbf{w}_{1,k}s_{1,k}$ and $\sum_{i,i\neq 1} \mathbf{h}_{i,k}\mathbf{x}_i$ in Eq. (15)) need to be obtained. Specifically, we can analyze the SINR distribution of SIC receiver. The amplitude of received signal in each antenna is the summation of multiple Rayleigh distributions. Based on [32], the PDF of the amplitude of received signal in each antenna follows the Nakagami distribution. Hence, the RSS (the square of received signal amplitude) distribution in each antenna follows Gamma distribution. After obtaining the RSS distributions, we can follow the similar approach in Appendix A of the supplemental material to obtain the successful decoding probability of SIC receiver. Following a similar analysis as Sec. 5, we then obtain the throughput of each link.

7 Practical Issues and TS Optimization

So far, we assume a TS is given and presented the detailed steps of the transmission phase of the proposed MAC protocol in Sec. 4.2. Under a given TS, we also analyzed the throughput of each link for the proposed MAC protocol in Sec. 5. In this section, we first discuss how to obtain the required information about each CTS through a training phase, and then use this information as the input to obtain an optimal TS that satisfies a specific network-wide objective (throughput and fairness). We introduce a training phase before transmissions.

7.1 Overview of Two Phases in MAC Protocol Implementation

The proposed protocol implementation includes two phases: training phase and transmission phase, as shown in Fig. 8.

Training phase: the goal of the training phase is to collect information for optimizing the transmission strategies among cross-technology networks. Such information includes the SIC decoding performance of each link under every possible CTS that involves itself. To gather such information, we design a training phase protocol to explore all CTSes in a round-robin fashion. Then, all transmitting nodes can determine the optimal TS that achieves a specific network-wide objective. An optimal TS is conducted in the transmission phase later.

Transmission phase: all LAA/WiFi links follow the optimal TS obtained from training phase for actual concurrent transmissions. The detailed steps of the transmission phase have been presented in Sec. 4.2.

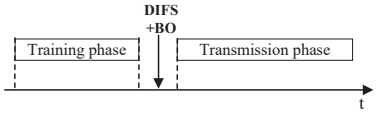

Fig. 8: Two phases of proposed MAC protocol.

7.2 Detailed Steps in Training Phase

Obtaining the optimal TS in the training phase requires the observations of successful decoding probabilities of links in all possible CTSes. Even though they may be obtained by having each link exchanging the decoding results of interested signals (success or failure) with all the other links (cross-technology communication), this will incur huge overhead in practice. For each link, we propose to implicitly infer the successful decoding probability for other links by monitoring the number of transmitted new packets and the number of re-transmitted packets of other links without decoding the unknown signals from different

technology. Based on this information, each transmitting node can build the concurrent transmission set profile and obtain the optimal TS.

However, the first problem we need to address is that LAA BS and WiFi AP need to identify transmitters even though there are multiple concurrent transmission links. We exploit the characteristic that each signal (either WiFi signal or LAA signal) carries a unique and static signature which can be used to identify different WiFi APs and LAA base stations. In this way, the sensing LAA base stations and WiFi APs can attribute the receiving signal to a specific transmitter upon receiving a signal.

7.2.1 WiFi AP Identifies Different LAA Base Stations

WiFi AP can detect LTE frames by cyclic prefix (CP)-based method [33]. The basic idea is that the WiFi AP set two capture windows W_1 and W_2 with fixed separation which is calculated based on the LTE standard [5], to capture LTE I/Q samples. WiFi AP shifts the two windows simultaneously by one sample at a time and keeps the window separation fixed. WiFi AP then calculates the correlations of the samples within these two windows and compares the correlation value with a threshold. If the correlation is higher than this threshold, it indicates LTE frame is detected. Note that, the CP-based method does not require WiFi AP to directly decode the LTE CP symbols. It utilizes the fact that CP symbols are the replication of a small portion of LTE data symbols and they repeatedly appear in LTE frames.

To help WiFi AP identify different LTE base stations, we can exploit the similar method by correlating the samples of the detected LTE frames with the saved signal signature of each LTE BS. This has been experimentally demonstrated in [34]. It utilizes the fact that primary synchronization signal (PSS) and secondary synchronization signal (SSS) can be deemed as the signal signature of an LTE BS.

7.2.2 LAA Base Station Identifies Different WiFi APs

Similarly, the LAA base station can obtain the signal signature of different WiFi APs by sampling the MAC address locations of WiFi frames. This is because each WiFi AP has a unique MAC address. For downlink transmissions of WiFi networks (WiFi AP to WiFi stations), as shown in Fig. 9, the address 1 stands for the MAC address of the intended receiver, the address 2 indicates the basic service set identifiers (BSSID) which is the MAC address of WiFi AP, address 3 indicates the source MAC address, which is the same as address 2 for downlink transmissions.

Frame Control	Duration /ID	Address 1	Address 2	Address 3	Sequence Control	Address 4	QoS Control	HT Control	Frame Body	FCS

Fig. 9: MAC header in 802.11 MAC frame.

We can exploit this fact to detect the WiFi frame, similar to Sec. 7.2.1. The main idea is to set two detection windows W_1 and W_2 of length L_{AP} which is the duration of MAC address of WiFi AP. The separation of W_1 and W_2 is set as 0 since address 2 and address 3 are nearby as shown in Fig. 9. Since each WiFi AP has a unique MAC address, similar as the process of how WiFi AP identifies new LTE transmitters, LAA base station can also identify if there is a new transmitter (WiFi AP) by correlating the signature of the newly received waveform with the stored signal signatures.

7.2.3 Exploring all CTSes

To infer the successful decoding probabilities for all CTSes, it is crucial for WiFi AP and LAA BS to identify if the received signal from a specific transmitter is being re-transmitted or a new signal. This can be done by sampling the received waveform starting from a fixed sample index (e.g., Ind_0) till the end of the received waveform. These samples can be saved as the signature of the received waveform. If the samples of the newly received waveform exhibit a high correlation with the previously saved signature, it indicates the newly received waveform is re-transmitted. This similar idea has also been experimentally demonstrated in [34].

All transmitting nodes need to explore the successful decoding probabilities of all CTSes. For the N LAA/WiFi coexistence links scenario, there are $2^N - 1$ CTS combinations in total. To efficiently explore all the CTSes and reduce the training time, we let LAA base stations and WiFi APs transmit short probing packets during the training phase. If the transmission is unsuccessful, it will be re-transmitted; if the transmission is successful, the corresponding transmitter will generate a new probing packet. We divide the training phase into multiple slots, which are further grouped into M rounds, where each round is the same.

The high-level idea of exploring CTSes is that each link first contends the shared channel. During the first N time slots, only the winning link can access the channel and other links avoid the collision with it. Then each link is attributed a unique access number, which is denoted as n_k for link k. After N slots, each link concurrently transmits with other links in a predefined order according to n_k. We show an example in Fig. 10 for $N = 3$ links. As we can see, the link whose $n_k = 1$ can transmit at slot t_1, t_4, t_5, t_7, the transmission time slots for link 2 and link 3 can also be calculated similarly. Since there are $2^N - 1$ CTSes, each training round consists of $2^N - 1$ slots.

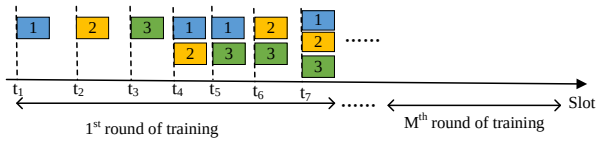

Fig. 10: Procedure of profiling CTSes for $N = 3$ links.

In each slot, each link can determine if its transmission is successful or not by ACK. If link k receives an ACK, then its transmission is successful. However, link k also needs to identify whether the transmissions of other links are successful or not. This can be done by the cross-correlation method presented in the beginning of this section to determine the re-transmission of other links.

For the whole M training rounds, for CTS_i, if link $k \in \text{CTS}_i$ observes there are $r_{k'}$ re-transmissions for link $k' \in \text{CTS}_i$, it estimates the successful decoding probability of link k' as:

$$p^s_{\text{CTS}_i}(k') = 1 - \frac{r_{k'}}{M}. \tag{17}$$

In fact, the above offline training phase can be viewed as a basic version of the explore-then-commit (ETC) algorithm in online learning. The idea of ETC is that, it explores all possible actions in a round-robin fashion for M time steps, then commits to the optimal learned action for the remaining time steps. If M is fixed, ETC's expected regret (difference of expected cumulative reward between the actions chosen in the online algorithm and the best action in hindsight) is linear. When M can be optimized according to the total time horizon T, ETC achieves expected regret $E[R(T)] \leq T^{\frac{2}{3}} \times O(K \log(T))^{\frac{1}{3}}$ [35] for T rounds.

7.3 TS Optimization in Training Phase

In this subsection, we show the transmission strategy optimization under different objectives in the training phase. Generally, we consider two types of objectives that are commonly discussed in the literature [36], [37]: throughput and fairness. From a system perspective, due to the shortage of frequency bands, to efficiently make use of the channel, achieving the maximum total throughput is desired. On the other hand, from the perspective of each link, it desires to deliver as much data as possible, this issue is related to fairness. We use the max-min individual throughput as the metric of fairness, which has been commonly used in [36], [37].

For the N links coexistence scenario, we denote the q-th transmission strategy as $\text{TS}_q, q = 1, 2, \cdots, B_N$. For each TS, we can theoretically obtain the normalized throughput of all LAA and WiFi links according to Sec. 5.

Maximize the total normalized throughput: Denote the total normalized throughput of TS_q as $\text{thr}_{\text{TS}_q}^{\text{total}}$, which is the summation of normalized throughput of all LAA and WiFi links under transmission strategy TS_q. We can easily formulate the maximization of total normalized throughput as:

$$\max_{\mathbf{a}} \quad a_q \cdot \text{thr}_{\text{TS}_q}^{\text{total}}, q \in \{1, 2, \cdots, B_N\}, \tag{18}$$

where $\mathbf{a} = [a_1, a_2, \cdots, a_{B_N}]$ is the decision variable vector, and $a_q = 1$ if the q-th TS is selected , $a_q = 0$ otherwise. In order to achieve this objective, the TS with the maximum total throughput is chosen to conduct the concurrent transmission MAC protocol.

Maximize the minimum individual normalized throughput: Denote $\text{thr}_{\text{TS}_q}(k)$ as the normalized throughput of link $k, k \in \mathcal{N}$ under transmission strategy TS_q. The optimization problem of maximizing the minimum individual normalized throughput is formulated as:

$$\max_{\mathbf{a}} \min_{k} \quad a_q \cdot \{\text{thr}_{\text{TS}_q}(k), k \in \mathcal{N}\}, \tag{19}$$

where $\mathbf{a}$ is the same as in Eq. (18). Then we select the optimal TS by solving the optimization problem in Eq. (19) to conduct concurrent transmission MAC protocol.

7.4 Computation and Training Overhead

We first analyze the computation overhead of SIC decoding. Denote the SIC decoding order as $\{l_1 > l_2 > \cdots > l_k > l\}$, where link l is the desired signal and there are k links that need to be decoded before link l. However, as the Rx of link l does not know which signal is the strongest, it blindly decodes signals to find out the correct SIC decoding order. On average, obtaining the correct SIC decoding order needs $\frac{k+1}{2}$ number of trials to identify and decode the strongest signal, and $\frac{k}{2}$ number of trials to decode the second strongest signal. The above processes are continued until link l's signal is decoded. In summary, the proposed SIC receivers on average need $\sum_{i=1}^{k} \frac{i+1}{2}$ number of trials. Using the above formula, for $k = 3, 4, 5$, SIC receivers on average need 4.5, 7, and 10 trials, respectively.

Next, we present SIC decoding latency analysis. Denote the average decoding and reconstructing latency of SIC receivers as $\bar{t}_d$ and $\bar{t}_c$, respectively. To obtain these values, we decode and reconstruct LTE, WiFi packets through MATLAB 2022a and record the CPU running time under Intel i9-10900K platform. The CPU running time is shown in Fig. 2 of the supplemental material, where $t_{\text{LTE},d}$ and $t_{\text{LTE},c}$ represent the latency of decoding and reconstructing an LTE packet. Averaging $t_{\text{LTE},d}$ and $t_{\text{WiFi},d}$ for all packets, we obtain $\bar{t}_d = 0.198$ seconds. Similarly, averaging $t_{\text{LTE},c}$ and $t_{\text{WiFi},c}$ for all packets, we obtain $\bar{t}_c = 0.028$ seconds. Therefore, the proposed SIC receivers on average bring $\sum_{i=1}^{k} \frac{i+1}{2}(\bar{t}_d + \bar{t}_c)$ decoding latency. The average latency are 1.017 seconds, 1.582 seconds, and 2.26 seconds, for $k = 3, 4, 5$, respectively. The decoding latency can be reduced if the SIC receiver is implemented on real transceiver hardware (e.g., FPGA).

Next, we analyze the training time of our protocol. For the N link coexistence scenario, since there are $2^N - 1$ mini-slots in each training round and there are M training rounds, the training overhead is $M(2^N - 1)T_{probe}$, where T_{probe} is the duration of probe packets during the training phase. Probe packet size ranges from 100 to 1400 Bytes [38], for probe packet size of 200 bytes and data rate of 21.7 Mbps, $T_{probe} \approx 0.07$ ms, which is significantly smaller than TXOP_{WiFi} (e.g., 1.5 ms) or TXOP_{LTE} (e.g., 2 ms). It can be further reduced with higher data rates and less probe packet size. For $M = 100$ and $T_{probe} \approx 0.07$ ms, the training latency of our protocol are 0.049 seconds, 0.105 seconds, and 0.217 seconds, respectively for $N = 3, 4, 5$.

7.5 Decoding Process of MU-MIMO with SIC

In this subsection, we discuss how a SIC receiver can decode the multi-user signals from super links that have stronger RSS than that from its own transmitter.

We start with a toy example shown in Fig. 7, assuming that super link 2 is the strongest signal and super link 1 is the second-strongest signal received at WiFi STA $k \in \mathcal{S}_1$. Namely, the SIC decoding order for WiFi STA $k, k \in \mathcal{S}_1$ should be: decoding super link 2 first, then decoding super link 1 to obtain its desired signal. Based on Eq. (15), we express y_k as:

$$y_k = \mathbf{h}_{2,k}\mathbf{x}_2 + I + n_{1,k}, \tag{20}$$

where $\mathbf{x}_2 \in \mathbb{C}^{M \times 1}, \mathbf{x}_2 = \sum_{l \in \mathcal{S}_2} \mathbf{w}_{2,l} s_{2,l}$. I is the total received signal from other transmitters. If $\mathbf{w}_{2,l}, l \in \mathcal{S}_2$, $\mathbf{h}_{2,k}$, and modulation scheme of super link 2 are known at WiFi STA $k, k \in \mathcal{S}_1$. WiFi STA k can estimate $s_{2,l}, l \in \mathcal{S}_2$ by minimizing the distance of y_k and the estimated symbols:

$$[\hat{s}_{2,l}]_{l=1}^{\mathcal{S}_2} = \underset{[s_{2,l} \in C_{2,l}]_{l=1}^{\mathcal{S}_2}}{\arg\min} |y_k - \mathbf{h}_{2,k} \sum_{l \in \mathcal{S}_2} \mathbf{w}_{2,l} s_{2,l}|, \tag{21}$$

where $C_{2,l}$ is the constellation set of symbols $s_{2,l}$. After that, the SIC receiver reconstruct and cancel out the interference from super link 2, until the desired signals are decoded.

In the above, we assume that the precoding vectors (e.g., $\mathbf{w}_{2,l}, l \in \mathcal{S}_2$) are known, which can be calculated by ZFBF rule if the internal channel state information within super link 2 can be obtained by WiFi STA $k, k \in \mathcal{S}_1$. Therefore, cross-channel state information (e.g., $\mathbf{h}_{2,k}$) and internal channel state information within super link 2 are needed for MU-MIMO SIC decoding, which can be obtained in practice via cross-technology communications [39].

7.6 Handling Unsaturated Traffic and Node Churn

In the saturated traffic case, all nodes have packets to transmit and participate in channel contention. Therefore, CTSes and TS do not need to change. In the unsaturated traffic case, if a node (e.g., a phone) does not have packets to transmit, it will not participate in the channel contention. However, if one CTS wins the channel contention and some nodes do not have packets, those nodes will keep being idle, which brings less interference to other links within the same CTS. Therefore, our MAC protocol can still work in this case. Yet, adopting a TS that is optimized under the saturated traffic case may not be optimal for unsaturated traffic. Alternatively, we can dynamically update the CTSes if we know the queue status of every node, but traffic is not fully predictable and incurs additional overhead.

In case of node joining or leaving, CTSes and TSes need to be updated. When a new node joins, existing nodes can implicitly discover new WiFi/LTE links without decoding, utilizing correlation-based signal detection techniques mentioned in Sec. 7.2. That is, a new signal signature will be observed from a new LTE node's PSS and SSS signals, and its ID will be added to the local database. Similarly, each node can discover new WiFi links by cross-correlation. On the other hand, if a node leaves, other nodes are able to detect the leaving nodes by checking the most recent time stamp that existing links were detected using cross-correlation. Only the CTSes involving the new link will need to be re-trained. Therefore, the CTSes and TSes for the new topology can be updated.

We remark that the proposed MAC protocol is compatible with the existing standards. Our protocol utilizes PHY-layer information (e.g., CSI, RSS, correlation) that is directly extractable from the PHY-layer of existing protocol standards. For example, correlation-based signal detection techniques can be adopted to implicitly estimate the operational parameters (e.g., differentiating WiFi/LTE links and discovering new WiFi/LTE links) of cross-technology transmissions without decoding, which is implemented in [34]. Our MAC protocol can be viewed as an extension to CSMA-CA since it retains the contention feature. The key difference is that, in our protocol, after channel contention is done, other links independently decide if they access the channel with the ongoing transmission or not. Whereas in CSMA-CA, the CTS reduces to a single link.

8 Simulation Results

In this section, we validate the theoretical analysis through extensive simulations. We simulate the LAA/WiFi coexistence in MATLAB according to their respective standards as shown in Table 1. For the channel of each link, we adopt the Rayleigh channel model. The power density of Gaussian noise is -90 dBm and the SINR threshold for successful decoding is set as 10 dB. The locations of transmitter and receiver for each LAA/WiFi link are uniformly generated within a 100×100 meter squared area.

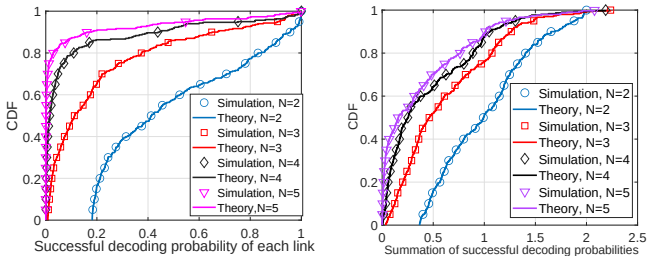

(a) CDF of successful decoding probability of each link.

(b) CDF of the total successful decoding probabilities of all links.

Fig. 11: CDF of simulation and theoretical results for successful decoding probability.

8.1 Validation of Successful Decoding Probabilities

It has been empirically shown that the number of concurrent transmission links (denoted by N) is no more than 5 in a collision domain in practice [16]. For SIC, the successful decoding probability performance diminishes as N increases [25], [26]. Even though the successful decoding probability derivation in Section 5.2 can be applied to any N, for demonstration and practical consideration, we only present the theoretical and simulation results of successful decoding probabilities for $N = 2, 3, 4, 5$.

In Fig. 11, we show the cumulative distribution function (CDF) of simulation and theoretical results for successful decoding probability, where 700 random LAA/WiFi coexistence topologies are generated. We can see that the theoretical results of successful decoding probability match with simulations under different N. In the meantime, when N increases, the successful decoding probability decreases rapidly due to more interference at the receiver. Fig. 11(b) depicts the CDF of summation of successful decoding probabilities for all N links. In the collision avoidance scheme, only one link is transmitting at each time slot. The summation of successful decoding probabilities of all links is around 1, if we ignore collisions and other interference. Therefore, for concurrent transmission cases, if the total successful decoding probability for all links is greater than 1, concurrent transmissions intuitively can potentially improve the total throughput. From 11(b), we can see that around 50%, 25% LAA/WiFi coexistence topologies can potentially bring improvement of total throughput for $N = 2$, $N = 3$, respectively. However, for $N = 4, 5$, the percentage is only around 10%.

8.2 Impact of M on Training Performance

We show the impact of the number of training rounds M on the estimation of successful decoding probability in Fig. 12. We use the relative variance to measure its impact. Specifically, assume there are L random topologies

of N LAA/WiFi coexistence links, the relative variance of estimating successful decoding probability is obtained by:

$$\text{var}(M) = \frac{\sum_{l=1}^{L}\sum_{i=1}^{N}\sum_{t=1}^{M}(\frac{x_{l,i,t}-\mathbb{E}[x_{l,i,t}]}{\mathbb{E}[x_{l,i,t}]})^2}{LNM} \quad (22)$$

Where $x_{l,i,t}$ is the estimation of successful decoding probability of link i for training round t under topology l.

From Fig. 12, we can see that as M increases, the relative variance decreases with the order of $O(\frac{1}{M})$, as indicated by Eq. (22) and [40]. We also notice that as N increases, the relative variance also quickly increases since the successful decoding probability of each link becomes smaller and more difficult to be estimated.

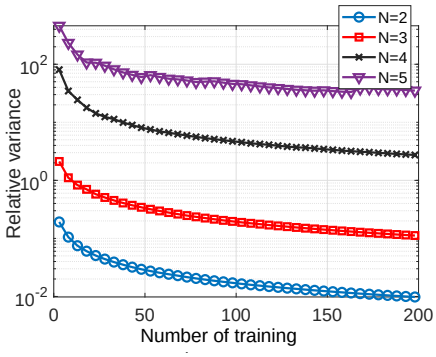

Fig. 12: Relative variance vs. training round M.

8.3 Normalized Throughput

8.3.1 Impact of N

We present the comparison of the normalized throughput for both simulations and theoretical analysis (obtained in Section 5.4) under $N = 2, 3, 4, 5$, choosing the TS shown in Table 4. In Fig. 13, we show the CDF of simulation and theoretical results for link throughput. We can see that the theoretical results match well with simulations under different N. In Fig. 13(d), we omit the results for link 2 and link 4 since link 2 has the same result as link 3, and link 4 has the same result as link 1.

8.3.2 Impact of Transmission Strategies

We validate the normalized throughput for different TSes. For demonstration, we show $N = 4$, with link setting the same as Table 4. Since there are $B_4 = 15$ TSes according to Eq. (4) for $N = 4$, We validate other four types of TS as shown in Table 3 besides the one (i.e., $\{\{1, 2\}, \{3\}, \{4\}\}$) that we have validated in Sec. 8.3.1.

As shown in Fig. 14, the theoretical throughput matches well with simulation for all different types of TS. For simplicity, we only show partial link throughput for each TS if some links have similar results. For example, in Fig. 14(b), link 1 has the similar result as link 4, link 2 has the similar result as link 3. TS_1 is the traditional collision avoidance scheme, indicating our theoretical model extends traditional collision avoidance scheme to concurrent transmission framework.

By varying different N and different transmission strategies, we show that the theoretical results generally match with simulations, which validates the theoretical throughput analysis.

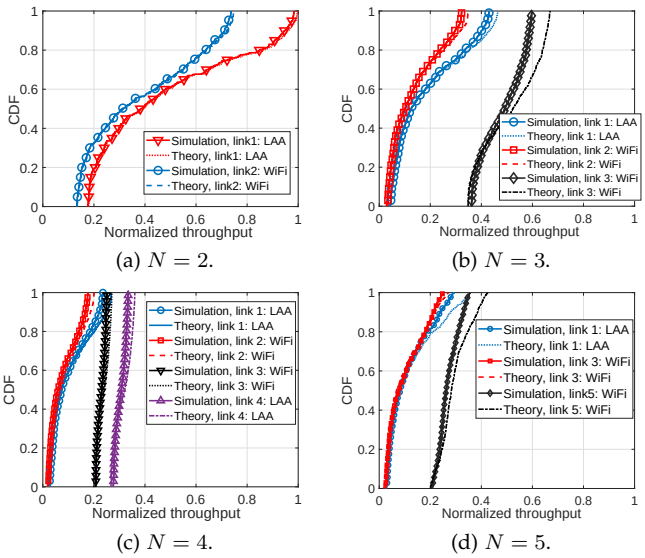

(a) $N = 2$. (b) $N = 3$.

(c) $N = 4$. (d) $N = 5$.

Fig. 13: CDF of simulation and theoretical results for link throughput for multi-link coexistence ($N = 2, 3, 4, 5$).

TABLE 3: Other four types of TS for four links coexistence.

Index of TS	Components
TS_1	{{1 }, { 2}, {3}, {4 } }
TS_2	{{1, 2}, {3, 4 } }
TS_3	{{1, 2, 3 }, {4 } }
TS_4	{ {1, 2, 3, 4 } }

8.4 Performance Comparisons

In this section, we compare the performance benefit of the proposed MAC protocol over two other MAC protocols (benchmarks). Benchmark 1 is the existing MAC protocol (i.e., CSMA-CA), benchmark 2 is only used to present the performance improvement of SIC over no SIC scheme. The performance measurements are network objectives (e.g., total throughput and minimum link throughput).

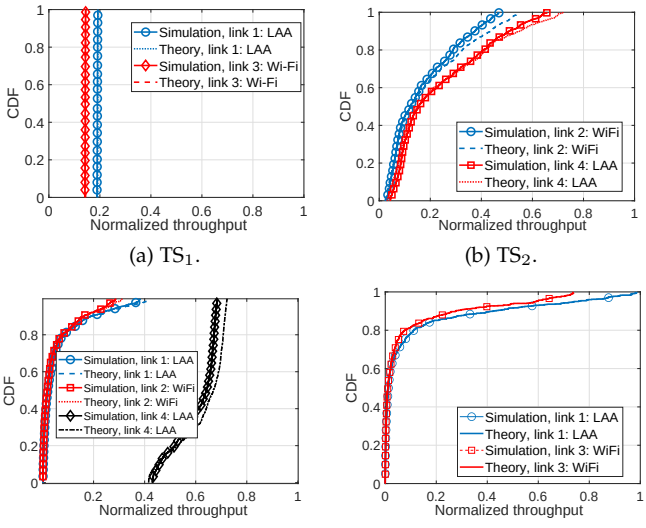

(a) TS_1. (b) TS_2.

(c) TS_3. (d) TS_4.

Fig. 14: CDF of simulation and theoretical results for link throughput, for different TSes.

TABLE 4: Simulated transmission strategies.

N	Selected TS	Link setting
2	{{1,2} }	(1,2)=(LAA, WiFi)
3	{{1,2}, {3} }	(1,2,3)=(LAA, WiFi, WiFi)
4	{{1,2}, { 3 }, {4 } }	(1,2,3,4)=(LAA, WiFi, WiFi, LAA)
5	{{1,2}, {3,4}, { 5} }	(1,2,3,4,5)=(LAA, WiFi,WiFi, LAA, WiFi)

- Benchmark 1 : CSMA-CA, commonly used in WiFi and LAA system.
- Benchmark 2 : optimal concurrent transmission with capture effect only (no SIC), abbreviated as OCT-CE. Transmitters select the optimal TS to achieve the corresponding network objective, but receivers decode signals without SIC.

Fig. 15 shows the performance comparison of three MAC protocols under different N. The link setting is still the same as that shown in the last column of Table 4. However, we choose the optimal TS in concurrent transmission MAC protocol. We do not show the results for $N = 5$, since they have similar trends as $N = 4$.

The performance of CSMA-CA is almost the same for all scenarios shown in Fig. 15, since in each scenario ($N = 2, 3, 4$), there are no concurrent transmissions for CSMA-CA, and the topology difference does not impact the throughput. Furthermore, we can observe that our proposed MAC protocol always outperforms benchmarks. There is the biggest performance gap between the proposed MAC protocol with OCT-CE for $N = 2$ because fewer concurrent transmission links lead to higher total successful decoding probabilities for the SIC receiver.

For the proposed MAC protocol, it can be noticed the optimal TS is highly likely to maximize the two objectives at the same time for $N = 2, 3$. This is because there are limited candidate TSes ($B_2 = 2, B_3 = 5$) to be chosen. Additionally, we can see in Fig. 15 that the max-min link throughput objective brings less total throughput, while it brings higher minimum link throughput, compared with max-total throughput objective. This is expected when we design the optimal MAC protocol to reach one specific objective. It is also interesting to notice that in Fig. 15(b)(d)(f), to reach the max-min throughput objective, OCT-CE tends to act similarly as CSMA-CA. However, the proposed MAC protocol can still find an optimal TS, which greatly outperforms OCT-CE and CSMA-CA.

8.5 MU-MIMO Performance

First, we validate the feasibility of MU-MIMO with SIC using simulation. Fig. 16(a) shows the successful decoding rate of MU-MIMO with SIC under different modulation schemes and power gaps for the scenarios of two concurrently transmitting super-links. The power gap is defined as the ratio of the strongest RSS among other super links to the total RSS of the remaining signals (i.e., intended signal has less RSS than the strongest interfering signal). We can see that the successful decoding rate increases with the power gap. In addition, higher modulation orders and more users in each super link degrade the decoding performance of MU-MIMO with SIC, since they bring a larger search space for the decoding symbols. Fig. 16(b) shows the decoding

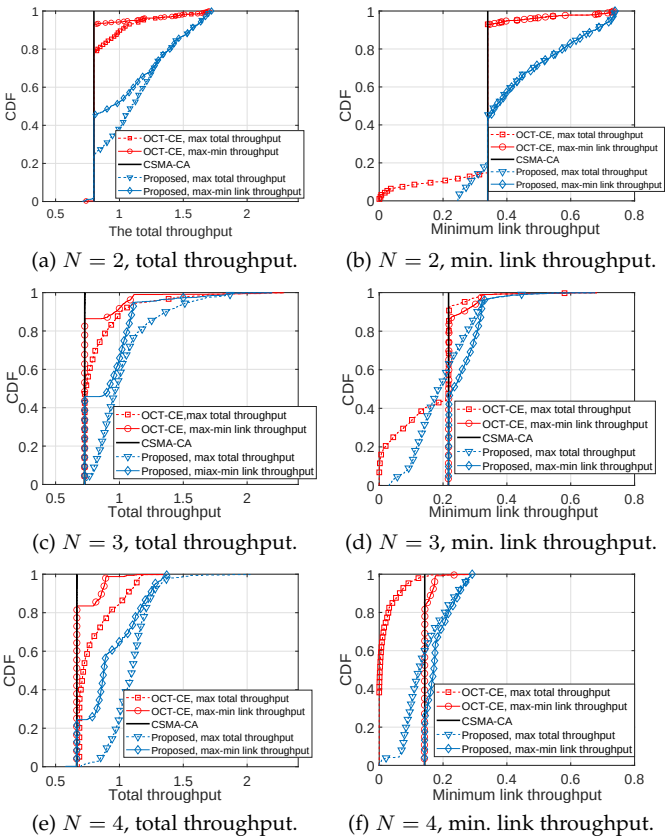

(a) $N = 2$, total throughput. (b) $N = 2$, min. link throughput.

(c) $N = 3$, total throughput. (d) $N = 3$, min. link throughput.

(e) $N = 4$, total throughput. (f) $N = 4$, min. link throughput.

Fig. 15: Performance of different MAC protocols.

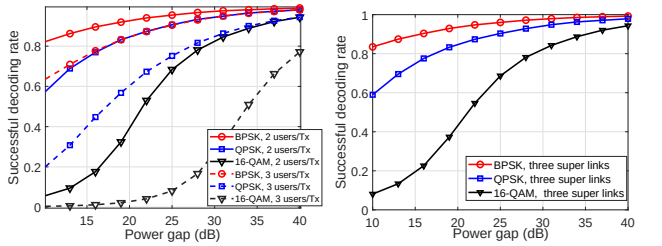

(a) Two super links concurrently transmit.

(b) Three super links concurrently transmit, where each super link has two users

Fig. 16: Successful decoding rate of MU-MIMO SIC.

performance under a three concurrent super-links scenario (each super link has two users). It achieves similar performances to the two super-links scenario under the same power gaps and modulation schemes.

We then present the results of comparison with MU-MIMO without SIC. For three-link concurrent transmissions, we consider 5 different transmission strategies (shown in Table 1 of supplemental material). Note that, for MU-MIMO without SIC (e.g., TS_5), we consider capture effect, which means successful decoding is possible when the RSS of interested signal is much stronger than interference under TS_5. In Fig. 17, we compare the objectives for different strategies. The CDF plots are obtained under 600 random coexistence topologies. We can see that MU-MIMO SIC always outperforms MU-MIMO without SIC. Comparing TS_1, TS_2, and TS_3, we know that $TS_1 < TS_3, TS_2 < TS_3$, this is because TS_3 creates two CTSes without any in-

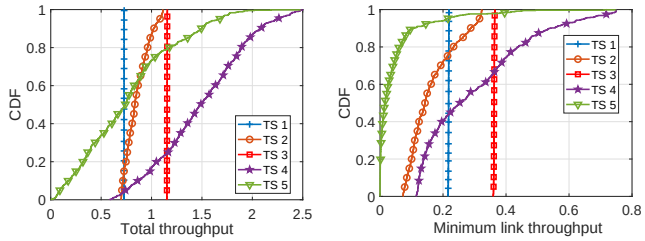

(a) Total throughput. (b) Minimum link throughput

Fig. 17: Performance comparison of network objectives for different transmission strategies shown in Table 1 of supplemental material, when $N = 3$.

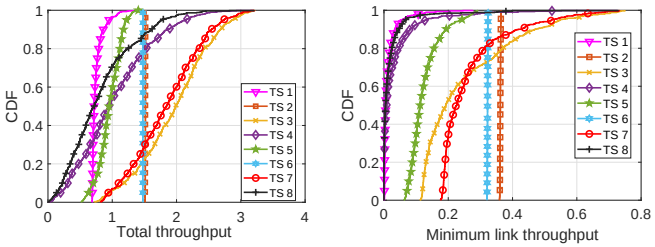

(a) Total throughput. (b) Minimum link throughput

Fig. 18: Performance comparison of network objectives for different transmission strategies shown in Table 2 of supplemental material, when $N = 4$.

terference between the two CTSes. Comparing TS_3 with TS_4, we know that TS_3 is sometimes better or worse than TS_4, this is determined by the interference between the two concurrently transmitting CTSes in TS_4. For four-link concurrent transmissions, the considered 8 transmission strategies are shown in Table 2 of supplemental material. In Fig. 18, similar trends can be observed for this case.

9 LAA/WiFi SIC Receiver Implementation

9.1 Overview and Methodology

To demonstrate the feasibility of SIC decoding for heterogeneous two-link LAA/WiFi coexistence, we implement a prototype SIC receiver with USRP devices. One LAA link concurrently transmits with one WiFi transmitter to the common SIC receiver. However, the same methodology can be applied to multi-link LAA/WiFi coexistence implementations, which are explained in Fig. 19. The basic idea is that, upon receiving the baseband waveform, the SIC receiver will first conduct either WiFi packet or LAA packet detection. Without loss of generality, we describe the process of WiFi packet detection first here. If the WiFi preamble CRC check passes, a valid WiFi packet is detected. Then the SIC receiver triggers the WiFi decoding module to decode WiFi payload bits. If the payload bits pass WiFi data CRC check, it means a WiFi packet is successfully decoded. SIC receiver proceeds to reconstruct the corresponding WiFi waveform by applying the channel effect. The reconstructed WiFi waveform is subtracted from the received waveform. SIC receiver then conducts LAA packet detection, if it identified a valid LAA base station cell ID, it will proceed to decode the LAA payloads bits, reconstruct LAA waveform, and cancel the reconstructed LAA waveform from the received waveform. The above process are iteratively conducted for iterative SIC decoding. If the received packet does not pass WiFi preamble/data CRC check and does not identify an LAA BS cell ID, it drops the current received packet and prepares to receive the next one.

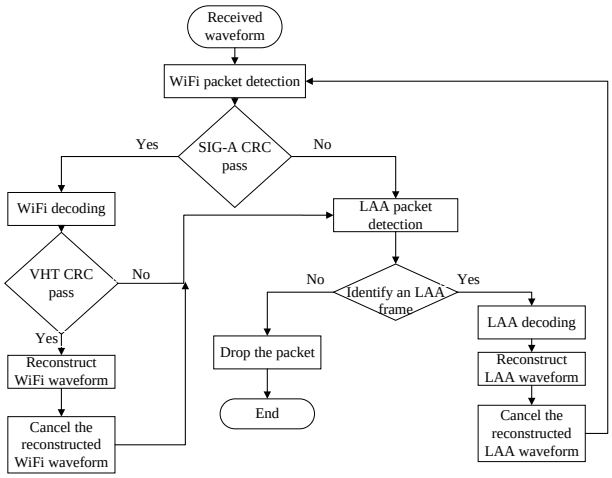

Fig. 19: General flowchart of proposed SIC implementation.

9.2 Key Components of SIC

9.2.1 WiFi Signal Decoding

The traditional WiFi decoding generally consists of time synchronization, frequency offset corrections, channel estimation and equalizing data symbols. To reconstruct WiFi waveform, it is critical to obtain the exact time-domain WiFi baseband I/Q samples. Therefore, phase tracking from symbol to symbol is needed by utilizing WiFi pilot subcarriers.

9.2.2 LAA Signal Decoding

Traditional LAA signal decoding includes frequency & time offset correction, PSS & SSS detection, and OFDM demodulation to obtain equalized data symbols. Different from the preamble in WiFi systems, reference symbols periodically appear in the LTE resource block (both time and frequency domain). Therefore, phase tracking and channel estimations for each symbol can be extracted to reconstruct exact time-domain LAA baseband waveform.

9.2.3 Reconstruction of WiFi/LAA Waveform

Fig. 20 shows the diagram of reconstructing WiFi/LAA waveform in the SIC receiver. To reconstruct WiFi/LAA waveform, WiFi (LAA) payload bits are firstly modulated to frequency symbols by OFDM modulation according to WiFi (LAA) transmission parameters. After that, in each subcarrier of WiFi (LAA), we multiply the estimated channel with the corresponding WiFi (LAA) OFDM symbol to imitate the channel effect on each subcarrier during transmissions. This makes sense considering the non-selective fading property for each subcarrier thanks to its narrow bandwidth. The channel-applied frequency symbols go through an inverse fast fourier transform (IFFT) operation to convert these symbols to time-domain samples. The reconstructed time-domain sample y' can then be obtained by parallel-to-series transformation and insert cyclic prefix (CP). Denote the

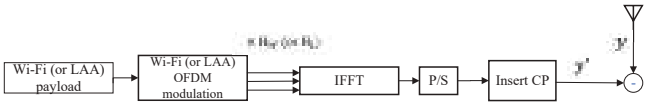

Fig. 20: Diagram of reconstructing WiFi/LAA waveform in SIC receiver.

received superimposed baseband time-domain signal as y. y' can be subtracted from y.

9.3 Experimental Results

To evaluate the performance of the SIC receiver and compare it with a conventional WiFi/LTE receiver, we created a real-world wireless communication testbed, where we used three (one LAA TX, one WiFi TX, one SIC receiver) National Instruments (NI) USRP 2921s to conduct over the air WiFi/LTE transmission and reception. We considered two topologies (see Figures 21 and 22), where we simultaneously transmit WiFi and LTE waveforms at 2.495 GHz [6]. We generated 802.11 ac waveforms with 20 MHz bandwidth and different MCS, using MATLAB's WLAN toolbox. For LTE, we generated LTE RC 2 Downlink RMC, using MATLAB's LTE toolbox. The SIC receiver received I/Q samples with a 20 Msps sampling rate, at the same frequency (i.e., 2.495 GHz) with LAA and WiFi transmitters.

In the first topology, both LTE and WiFi transmitters are 2.6 meters away from the receiver; whereas, in the second topology, LTE and WiFi transmitters are 5.9 meters and 3.8 meters away from the receiver, respectively.

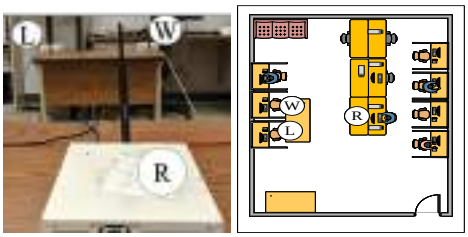

Fig. 21: Topology 1 floor map.

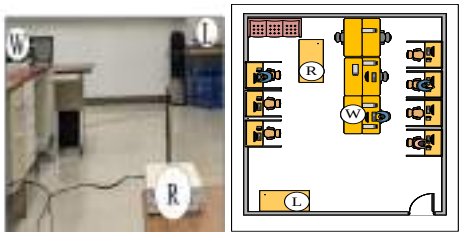

Fig. 22: Topology 2 floor map.

We define the following metrics to evaluate throughout our experiments:

- *WiFi frame detection rate:* the ratio of the number of detected WiFi frames over the total number of transmitted WiFi frames.
- *WiFi frame drop rate:* the ratio of the number of detected WiFi frames that failed data CRC check over the total number of detected WiFi frames.

6. We chose this frequency because it had the least transmission activity.

TABLE 5: SIC decoder performance improvement over WiFi and LTE decoders (topology 1).

SIR (dB)	WiFi detection rate	WiFi drop rate	WiFi BER	LTE BER
-10	$+533.31\%$	N/A	-99.77%	0%
-5	$+280.01\%$	N/A	-78.44%	0%
0	$+20\%$	-32.15%	-7.26%	-39.82%
5	0%	0%	0%	-80%
10	0%	0%	0%	-92.52%

TABLE 6: SIC decoder performance improvement over WiFi and LTE decoders (topology 2).

SIR (dB)	WiFi detection rate	WiFi drop rate	WiFi BER	LTE BER
-10	$+400\%$	N/A	-99.5%	0%
-5	$+499.88\%$	-49.48%	-52.94%	0%
0	$+27.26\%$	-28.45%	-26.31%	-35.77%
5	0%	0%	0%	-82.69%
10	0%	0%	0%	-89.22%

- *WiFi BER:* BER calculated over the transmitted payload of detected WiFi frames.
- *LTE BER:* BER calculated over transmitted payload of detected LTE frames.

To evaluate SIC under different ratios of received power for WiFi and LTE, we define signal-to-interference ratio (*SIR*) as $10\log(\frac{P_{\text{WiFi}}}{P_{\text{LTE}}})$, where P_{LTE} and P_{WiFi} are the received power of LTE and WiFi, respectively. To show performance results under different SIR settings, for each topology, we tune the appropriate TX gains applied at the transmitters to achieve desirable received SIR settings.

The WiFi frame detection rate vs. SIR for topology 1 and 2 are represented in Figures 23a and 24a, respectively. The performance improvement of the proposed SIC decoder over traditional WiFi and LTE decoders under different SIR values for topology 1 and 2 are shown in Tables 5 and 6. The '+' and '-' symbol represent that the performance of the proposed SIC receiver are increased and decreased, respectively. It can be seen that the SIC receiver performs as same as the WiFi receiver for positive SIR values, i.e., WiFi received power is higher. However, for non-positive SIR values, the SIC receiver improves detection rate by $3.8\times$ and $4.1\times$ on average for topology 1 and 2, respectively. Figures 23b and 24b depict the frame drop rate vs. SIR for the former typologies. As expected, the SIC receiver performs the same as the WiFi receiver for positive SIR values; whereas, over non-positive SIR values, SIC decreases frame drop rate by 11% and 26%, for topologies 1 and 2, respectively. BER vs. SIR results for WiFi, under topology 1 and 2, can be seen in Figures 23c and 24c, respectively. As before, BER performance results for positive SIR values are the same as a conventional WiFi receiver; however, over non-positive SIR values, SIC decreases BER 61.82%, 59.59%, compared to WiFi receiver, for topologies 1 and 2, respectively. Finally, Figures 23d and 24d depict BER vs. SIR for LTE, under SIC and conventional LTE receivers, for topology 1 and 2, respectively. In this case, SIC brings same BER results as an LTE receiver for negative SIR values. However, over non-negative SIR values, SIC decreases LTE BER results by 70.78% and 69.22%, compared to a conventional LTE receiver, for topology 1 and 2, respectively.

It can be concluded that under both topologies, the SIC receiver improves the performances, compared with conventional WiFi and LTE receiver, when the intended signal has lower or equal power as the interfered signal.

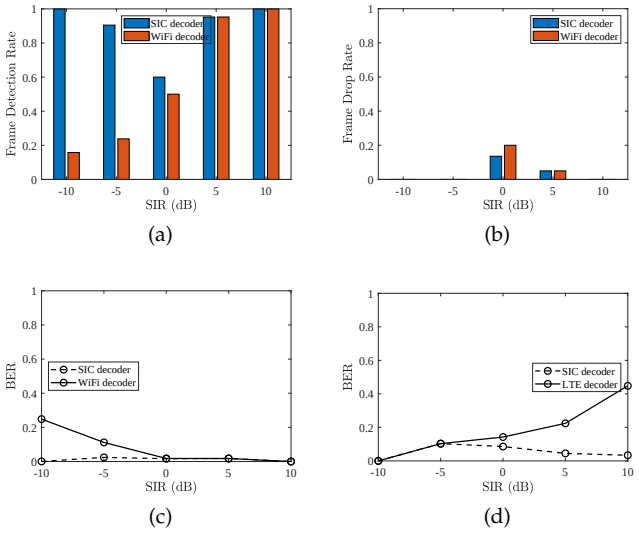

Fig. 23: (a) WiFi frame detection rate, (b) WiFi frame drop rate, (c) WiFi BER , and (d) LTE BER vs. SIR for Topology 1.

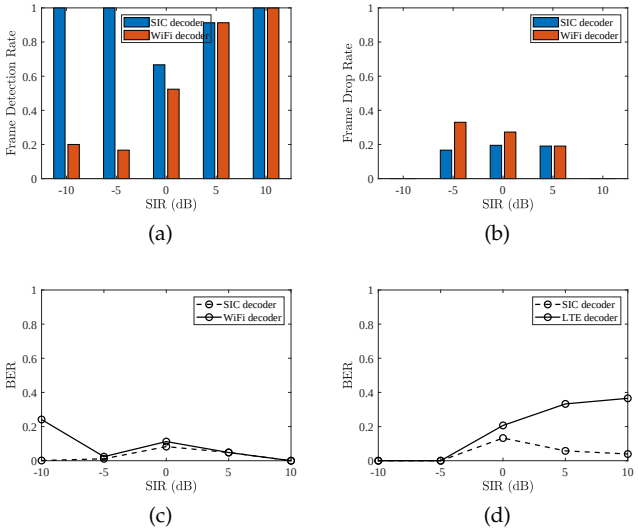

Fig. 24: (a) WiFi frame detection rate, (b) WiFi frame drop rate, (c) WiFi BER , and (d) LTE BER vs. SIR for Topology 2.

10 Conclusions

In this paper, we explore interference cancellation techniques to enhance coexistence of different technologies in unlicensed bands, using LTE and WiFi as a case study. We propose a SIC-aware MAC protocol that allows concurrent transmissions and optimizes the channel access strategy, which mitigates the cross-technology interference due to excessive channel contention caused by many coexisting links. We provide a theoretical analysis of the network throughput by generalizing the classical Bianchi model to consider CTS-level contentions and SIC techniques. We then discuss practical issues of implementing our MAC protocol. Simulation results show that our proposed MAC protocol can significantly improve the network throughput and fairness. We also implement a prototype SIC receiver for LAA/WiFi coexistence on USRP devices, to demonstrate its feasibility and performance benefits. As future work, we will explore efficient online learning algorithms to reduce the training phase of our protocol.

References

[1] "Revision of part 15 of the commission's rules to permit unlicensed national information infrastructure (U-NII) devices in the 5GHz band," Federal Commun. Commission, 2015.

[2] 3GPP, "NR-based access to unlicensed spectrum," Standard (TR) 36.889, 2019.

[3] Qualcomm. Extending LTE advanced to unlicensed spectrum. [Online]. Available: https://www.qualcomm.com/media/documents/files/white-paper-extending-lte-advanced-to-unlicensed-spectrum.pdf

[4] A. M. Cavalcante, E. Almeida, R. D. Vieira, S. Choudhury, E. Tuomaala, K. Doppler, F. Chaves, R. C. D. Paiva, and F. Abinader, "Performance evaluation of LTE and Wi-Fi coexistence in unlicensed bands," in *IEEE 77th Vehicular Technology Conference (VTC Spring)*, 2013, pp. 1–6.

[5] 3GPP, "Feasibility study on licensed-assisted access to unlicensed spectrum," Standard (TR) 36.889, 2015.

[6] "IEEE standard for information technology-telecommunications and information exchange between systems-local and metropolitan area networks-specific requirements-part 11: Wireless LAN medium access control (MAC) and physical layer (PHY) specifications," IEEE Standard 802.11, 2012.

[7] E. Magistretti, K. K. Chintalapudi, B. Radunovic, and R. Ramjee, "WiFi-Nano: Reclaiming WiFi efficiency through 800 ns slots," in *Proceedings of the 17th annual international conference on Mobile computing and networking*, 2011, pp. 37–48.

[8] G. Bianchi, "Performance analysis of the IEEE 802.11 distributed coordination function," *IEEE Journal on Selected Areas in Communications*, vol. 18, no. 3, pp. 535–547, 2000.

[9] Y. Gao, X. Chu, and J. Zhang, "Performance analysis of LAA and WiFi coexistence in unlicensed spectrum based on markov chain," in *IEEE Global Communications Conference (GLOBECOM)*, 2016, pp. 1–6.

[10] M. Mehrnoush, V. Sathya, S. Roy, and M. Ghosh, "Analytical modeling of Wi-Fi and LTE-LAA coexistence: Throughput and impact of energy detection threshold," *IEEE/ACM Transactions on Networking*, vol. 26, no. 4, pp. 1990–2003, 2018.

[11] A. M. Cavalcante, E. Almeida, R. D. Vieira, S. Choudhury, E. Tuomaala, K. Doppler, F. Chaves, R. C. D. Paiva, and F. Abinader, "Performance evaluation of LTE and Wi-Fi coexistence in unlicensed bands," in *IEEE 77th Vehicular Technology Conference (VTC Spring)*, 2013, pp. 1–6.

[12] A. M. Baswade, L. Beltramelli, F. A. Antony, M. Gidlund, B. R. Tamma, and L. Guntupalli, "Modelling and analysis of Wi-Fi and LAA coexistence with priority classes," in *14th International Conference on Wireless and Mobile Computing, Networking and Communications (WiMob)*, 2018, pp. 1–8.

[13] M. Hirzallah, Y. Xiao, and M. Krunz, "On modeling and optimizing LTE/Wi-Fi coexistence with prioritized traffic classes," in *IEEE International Symposium on Dynamic Spectrum Access Networks (DySPAN)*, 2018, pp. 1–10.

[14] R. Yin, G. Yu, A. Maaref, and G. Y. Li, "LBT-based adaptive channel access for LTE-U systems," *IEEE Transactions on Wireless Communications*, vol. 15, no. 10, pp. 6585–6597, 2016.

[15] G. J. Sutton, R. P. Liu, and Y. J. Guo, "Delay and reliability of load-based listen-before-talk in LAA," *IEEE Access*, vol. 6, pp. 6171–6182, 2018.

[16] Y. Xiao, M. Hirzallah, and M. Krunz, "Distributed resource allocation for network slicing over licensed and unlicensed bands," *IEEE Journal on Selected Areas in Communications*, vol. 36, no. 10, pp. 2260–2274, 2018.

[17] S. Gollakota, F. Adib, D. Katabi, and S. Seshan, "Clearing the RF smog: making 802.11n robust to cross-technology interference," in *Proceedings of the ACM SIGCOMM Conference*, 2011, pp. 170–181.

[18] Y. Hou, M. Li, X. Yuan, Y. T. Hou, and W. Lou, "Cooperative cross-technology interference mitigation for heterogeneous multi-hop networks," in *IEEE INFOCOM - IEEE Conference on Computer Communications*, 2014, pp. 880–888.

[19] P. Yang, Y. Yan, X.-Y. Li, Y. Zhang, Y. Tao, and L. You, "Taming cross-technology interference for Wi-Fi and ZigBee coexistence networks," *IEEE Transactions on Mobile Computing*, vol. 15, no. 4, pp. 1009–1021, 2016.

[20] Y. Yan, P. Yang, X.-Y. Li, Y. Zhang, J. Lu, L. You, J. Wang, J. Han, and Y. Xiong, "WizBee: Wise ZigBee coexistence via interference cancellation with single antenna," *IEEE Transactions on Mobile Computing*, vol. 14, no. 12, pp. 2590–2603, 2015.

[21] S. Yun and L. Qiu, "Supporting WiFi and LTE coexistence," in *IEEE Conference on Computer Communications (INFOCOM)*, 2015, pp. 810–818.

[22] S. Verdu *et al.*, *Multiuser detection*. Cambridge university press, 1998.

[23] K. C.-J. Lin, S. Gollakota, and D. Katabi, "Random access heterogeneous MIMO networks," *ACM SIGCOMM Computer Communication Review*, vol. 41, no. 4, pp. 146–157, 2011.

[24] R. A. Brualdi, *Introductory combinatorics*. Pearson Education India, 1977.

[25] M. Wildemeersch, T. Q. S. Quek, M. Kountouris, A. Rabbachin, and C. H. Slump, "Successive interference cancellation in heterogeneous networks," *IEEE Transactions on Communications*, vol. 62, no. 12, pp. 4440–4453, 2014.

[26] X. Zhang and M. Haenggi, "The performance of successive interference cancellation in random wireless networks," *IEEE Transactions on Information Theory*, vol. 60, no. 10, pp. 6368–6388, 2014.

[27] S. P. Weber, J. G. Andrews, X. Yang, and G. de Veciana, "Transmission capacity of wireless Ad Hoc networks with successive interference cancellation," *IEEE Transactions on Information Theory*, vol. 53, no. 8, pp. 2799–2814, 2007.

[28] Z. Guo, M. Li, and Y. Xiao, "Enhancing LAA/Wi-Fi coexistence via concurrent transmissions and interference cancellation," in *IEEE International Symposium on Dynamic Spectrum Access Networks (DySPAN)*, 2019, pp. 1–10.

[29] Z. ning Kong, D. Tsang, B. Bensaou, and D. Gao, "Performance analysis of IEEE 802.11e contention-based channel access," *IEEE Journal on Selected Areas in Communications*, vol. 22, no. 10, pp. 2095–2106, 2004.

[30] J. Lee, W. Kim, S.-J. Lee, D. Jo, J. Ryu, T. Kwon, and Y. Choi, "An experimental study on the capture effect in 802.11a networks," in *Proceedings of the second ACM international workshop on Wireless network testbeds, experimental evaluation and characterization*, 2007, pp. 19–26.

[31] S. Huang, H. Yin, J. Wu, and V. C. Leung, "User selection for multiuser MIMO downlink with zero-forcing beamforming," *IEEE Transactions on Vehicular Technology*, vol. 62, no. 7, pp. 3084–3097, 2013.

[32] J. Hu and N. C. Beaulieu, "Accurate simple closed-form approximations to Rayleigh sum distributions and densities," *IEEE Communications Letters*, vol. 9, no. 2, pp. 109–111, 2005.

[33] M. Hirzallah, W. Afifi, and M. Krunz, "Full-duplex-based rate/mode adaptation strategies for Wi-Fi/LTE-U coexistence: A POMDP approach," *IEEE Journal on Selected Areas in Communications*, vol. 35, no. 1, pp. 20–29, 2017.

[34] I. Samy, X. Han, L. Lazos, M. Li, Y. Xiao, and M. Krunz, "Misbehavior detection in Wi-Fi/LTE coexistence over unlicensed bands," *IEEE Transactions on Mobile Computing*, 2022.

[35] A. Slivkins *et al.*, "Introduction to multi-armed bandits," *Foundations and Trends® in Machine Learning*, vol. 12, no. 1-2, pp. 1–286, 2019.

[36] A. Doshi, S. Yerramalli, L. Ferrari, T. Yoo, and J. G. Andrews, "A deep reinforcement learning framework for contention-based spectrum sharing," *IEEE Journal on Selected Areas in Communications*, vol. 39, no. 8, pp. 2526–2540, 2021.

[37] Y. Yu, T. Wang, and S. C. Liew, "Deep reinforcement learning multiple access for heterogeneous wireless networks," *IEEE Journal on Selected Areas in Communications*, vol. 37, no. 6, pp. 1277–1290, 2019.

[38] N. Hu and P. Steenkiste, "Evaluation and characterization of available bandwidth probing techniques," *IEEE journal on Selected Areas in Communications*, vol. 21, no. 6, pp. 879–894, 2003.

[39] P. Gawlowicz, A. Zubow, and A. Wolisz, "Enabling cross-technology communication between LTE unlicensed and WiFi," in *IEEE Conference on Computer Communications (INFOCOM)*, 2018, pp. 144–152.

[40] S. Gupta and V. Kapoor, *Fundamentals of mathematical statistics*. Sultan Chand & Sons, 2020.

Zhiwu Guo received the B.S. and M.S. degrees in electrical and computer engineering from University of Electronic Science and Technology of China, in 2014 and in 2017, respectively. He is currently working towards the Ph.D. degree at the Department of Electrical and Computer Engineering, the University of Arizona. His research interests include heterogeneous network spectrum sharing, interference cancellation, and artificial intelligence for wireless communication and networking.

Ming Li (S'08-M'11-SM'17) is an Associate Professor in the Department of Electrical and Computer Engineering of University of Arizona, and also affiliated with the Computer Science Department. He was an Assistant Professor in the Computer Science Department at Utah State University from 2011 to 2015. He received his Ph.D. in ECE from Worcester Polytechnic Institute, MA, in 2011. His main research interests are wireless and cyber security, with current emphases on intelligent NextG wireless networks, wireless physical-layer security, privacy enhancing technologies, and cyber-physical system security. He has has published more than 120 journal articles and peer-reviewed conference papers, and his latest h-index is 40. He received the NSF Early Faculty Development (CAREER) Award in 2014, and the ONR Young Investigator Program (YIP) Award in 2016. He was a recipient of six paper awards, including the best paper award from ACM WiSec 2020. He has served/is serving on the editorial boards of IEEE TMC and TDSC. He was a TPC Co-chair of IEEE CNS 2022. He is a senior member of IEEE, and a member of ACM.

Marwan Krunz (S'93-M'95-SM'04-F'10) is a Regents Professor at the University of Arizona. He holds the Kenneth VonBehren Endowed Professorship in ECE and is also a professor of computer science. He directs the Broadband Wireless Access and Applications Center (BWAC), a multi-university NSF/industry center that focuses on next-generation wireless technologies. He also holds a courtesy appointment as a professor at University Technology Sydney. Previously, he served as the site director for the Connection One center. Dr. Krunz's research is on resource management, network protocols, and security for wireless systems. He has published more than 300 journal articles and peer-reviewed conference papers, and is a named inventor on 12 patents. His latest h-index is 60. He is an IEEE Fellow, an Arizona Engineering Faculty Fellow, and an IEEE Communications Society Distinguished Lecturer (2013-2015). He received the NSF CAREER award. He served as the Editor-in-Chief for the IEEE Transactions on Mobile Computing. He also served as editor for numerous IEEE journals. He was the TPC chair for INFOCOM'04, SECON'05, WoWMoM'06, and Hot Interconnects 9. He was the general vice-chair for WiOpt 2016 and general co-chair for WiSec'12. Dr. Krunz served as chief scientist for two startup companies that focus on 5G and beyond systems and machine learning for wireless communications.